J Math Chem (2014) 52:508–542
DOI 10.1007/s10910-013-0276-y

ORIGINAL PAPER

Symmetry-itemized enumeration of quadruplets of *RS*-stereoisomers: I—the fixed-point matrix method of the USCI approach combined with the stereoisogram approach

Shinsaku Fujita

Received: 21 September 2013 / Accepted: 12 October 2013 / Published online: 31 October 2013

Abstract The *RS*-stereoisomeric group $\mathbf{T}_{d\tilde{\sigma}\hat{I}}$ is examined to characterize quadruplets of *RS*-stereoisomers based on a tetrahedral skeleton and found to be isomorphic to the point group $\mathbf{O}_h$ of order 48. The non-redundant set of subgroups (SSG) of $\mathbf{T}_{d\tilde{\sigma}\hat{I}}$ is obtained by referring to the non-redundant SSG of $\mathbf{O}_h$. The coset representation for characterizing the orbit of the four positions of the tetrahedral skeleton is clarified to be $\mathbf{T}_{d\tilde{\sigma}\hat{I}}(/\mathbf{C}_{3v\tilde{\sigma}\hat{I}})$, which is closely related to the $\mathbf{O}_h(/\mathbf{D}_{3d})$. According to the unit-subduced-cycle-index (USCI) approach (Fujita in Symmetry and combinatorial enumeration in chemistry. Springer, Berlin, 1991), the subdution of $\mathbf{T}_{d\tilde{\sigma}\hat{I}}(/\mathbf{C}_{3v\tilde{\sigma}\hat{I}})$ is examined so as to generate unit subduced cycle indices with chirality fittingness (USCI-CFs). The fixed-point matrix method of the USCI approach is applied to the USCI-CFs. Thereby, the numbers of quadruplets are calculated in an itemized fashion with respect to the subgroups of $\mathbf{T}_{d\tilde{\sigma}\hat{I}}$. After the subgroups of $\mathbf{T}_{d\tilde{\sigma}\hat{I}}$ are categorized into types I–V, type-itemized enumeration of quadruplets is conducted to illustrate the versatility of the stereoisogram approach.

Keywords Stereoisogram · RS-stereoisomers · RS-stereoisomeric groups · Combinatorial enumeration · USCI approach

1 Introduction

The dichotomy between enantiomers and "diastereomers" [1] has scattered unconscious but serious confusion caused by a verbal transmutation of the term "diastereomers", as indicated from a chemical philological point of view [2]. This situation has not changed yet, so that the dichotomy is widely adopted as one of the fundamental

S. Fujita (✉)
Shonan Institute of Chemoinformatics and Mathematical Chemistry,
Kaneko 479-7 Ooimachi, Ashigara-Kami-Gun, Kanagawa-Ken 258-0019, Japan
e-mail: shinsaku_fujita@nifty.com

concepts in stereochemistry in most textbooks on organic stereochemistry [3–5] and on organic chemistry [6–10].

Because the conventional term "diastereomers" has no mathematical basis so as to contain rather indefinite connotation, the history of the Cahn, Ingold and Prelog (CIP) system [11,12] has shown confusion over chirality and stereogenicity. In a parallel way, the related method for giving pro-*R*/pro-*S*-descriptors [13] has shown confusion over prochirality and prostereogenicity.

On the basis of the proligand-promolecule model [14], the concept of *stereoisograms* has been proposed by the author (Fujita) to discuss stereogenicity and chirality comprehensively [15]. Thereby, it has been clarified that the conventional stereogenicity should be replaced by a more definite term, '*RS*-stereogenicity' for the purpose of comparing it with chirality [16]. Each stereoisogram consists of a quadruplet of *RS*-stereoisomers, i.e., a reference promolecule, an enantiomer, an *RS*-diastereomer, and a holantimer which is capable of comprehensive discussions on pseudoasymmetry, *RS*-stereogenicity, chirality and the Cahn-Ingold-Prelog system of *RS*-nomenclature [17–20] as well as on prochirality [21–25].

Such a quadruplet contained in a stereoisogram is governed by a newly-defined *RS*-stereoisomeric group. The *RS*-stereoisomeric groups and related groups have been constructed to discuss tetrahedral derivatives [16], allene derivatives [26,27], square-planar complexes [28], ethylene derivatives [29], trigonal bipyramidal compounds [30,31], and prismane derivatives [32,33]. The existence of five types of stereoisograms has been proven on the basis of the existence of five types of subgroups of *RS*-stereoisomeric groups [34]. The concept of *correlation diagrams of stereoisograms* has been proposed for the purpose of characterizing stereoisomers [35–37]. Methodologies for investigating geometric and stereoisomeric features in stereochemistry have been developed on the basis of the stereoisogram approach [38–40].

In addition to these reports on qualitative discussions, itemized enumeration of quadruplets of *RS*-stereoisomers under the action of *RS*-stereoisomeric groups has been reported [41], where the itemization is concerned with stereoisograms of Type I–V. For the purpose of comprehensive discussions, it is desirable to investigate more detailed itemization.

The author has recently reported symmetry-itemized enumeration of cubane derivatives [42,43], where the USCI (unit-subduced-cycle-index) approach [44–46] is applied to the $\mathbf{O}_h$-point group. Because the $\mathbf{O}_h$-point group is isomorphic to the *RS*-stereoisomeric group of tetrahedral compounds, the present report is devoted to investigate more detailed itemization of quadruplets of *RS*-stereoisomers.

2 *RS*-stereoisomeric groups

Let us first consider a tetrahedral skeleton **1** to introduce the concept of stereoisograms [15]. The skeleton **1** is controlled by a point group $\mathbf{T}_d$ (order 24), which can be extended into the corresponding *RS*-stereoisomeric group $\mathbf{T}_{d\tilde{\sigma}\hat{I}}$ (order 48).

The *RS*-stereoisomeric group $\mathbf{T}_{d\tilde{\sigma}\hat{I}}$ has a normal subgroup $\mathbf{T}$(order 12), which is also a normal subgroup of $\mathbf{T}_d$. Hence, the $\mathbf{T}_{d\tilde{\sigma}\hat{I}}$-group is decomposed into cosets as follows:

$$\mathbf{T}_{d\widetilde{\sigma}\widehat{I}} = \mathbf{T} + \sigma\mathbf{T} + \widetilde{\sigma}\mathbf{T} + \widehat{I}\mathbf{T}, \tag{1}$$

which has been noted previously (Eq. 8 of [41]). Note that the point group $\mathbf{T}_d$ for the reference tetrahedral skeleton is decomposed as follows:

$$\mathbf{T}_d = \mathbf{T} + \sigma\mathbf{T}, \tag{2}$$

where the symbol σ is a representative selected from the 12 reflection operations of $\mathbf{T}_d$. The coset decomposition shown by Eq. 2 characterizes an enantiomeric relationship.

In addition, there appears a subgroup of order 24 for characterizing an *RS*-diastereomeric relationship:

$$\mathbf{T}_{\widetilde{\sigma}} = \mathbf{T} + \widetilde{\sigma}\mathbf{T}, \tag{3}$$

which has been noted previously (Eq. 44 of [41]). Note that the symbol $\widetilde{\sigma}$ represents an operation which has the same permutation as σ but no alternation of chirality. Another subgroup of order 24 characterizes a holantimeric relationship:

$$\mathbf{T}_{\widehat{I}} = \mathbf{T} + \widehat{I}\mathbf{T}, \tag{4}$$

which has been noted previously (Eq. 57 of [41]). Note that the symbol $\widehat{I}$ represents an operation which has the same permutation as I but alternation of chirality.

The operations of $\mathbf{T}_{d\widetilde{\sigma}\widehat{I}}$ are summarized in the $\mathbf{T}_{d\widetilde{\sigma}\widehat{I}}$-columns of Table 1. The upper-left part marked by the gray letter **A** collects the operations of the normal subgroup **T**, the lower-left part marked by the gray letter **B** collects the operations of the coset $\sigma\mathbf{T}(= \mathbf{T}_d - \mathbf{T})$ (cf. Eq. 2), the upper-right part marked by the gray letter **C** collects the operations of the coset $\widetilde{\sigma}\mathbf{T}(= \mathbf{T}_{\widetilde{\sigma}} - \mathbf{T})$ (cf. Eq. 3), and the lower-right part marked by the gray letter **D** collects the operations of the coset $\widehat{I}\mathbf{T}(= \mathbf{T}_{\widehat{I}} - \mathbf{T})$ (cf. Eq. 4). Hence, Eqs. 1–4 are alternatively represented in the form of sets of operations:

$$\mathbf{T}_{d\widetilde{\sigma}\widehat{I}} = \{\mathbf{A}, \mathbf{B}, \mathbf{C}, \mathbf{D}\} \tag{5}$$

$$\mathbf{T}_d = \{\mathbf{A}, \mathbf{B}\} \tag{6}$$

$$\mathbf{T}_{\widetilde{\sigma}} = \{\mathbf{A}, \mathbf{C}\} \tag{7}$$

$$\mathbf{T}_{\widehat{I}} = \{\mathbf{A}, \mathbf{D}\} \tag{8}$$

$$\mathbf{T} = \{\mathbf{A}\}, \tag{9}$$

where the cosets **A**, **B**, **C**, and **D** (gray letters) contain the operations listed in the $\mathbf{T}_{d\widetilde{\sigma}\widehat{I}}$-columns of Table 1. It should be noted that each operation of **A** corresponds to an operation of **D**, where the correspondence is shown by the absence or presence of a hat accent. In a similar way, each operation of **B** corresponds to an operation of **C**, where the correspondence is shown by the absence or presence of a tilde accent.

Each of the four cosets shown in the right-hand side of Eq. 1 corresponds to one component of a quadruplet of *RS*-stereoisomers, i.e., **T** to a reference skeleton, $\sigma\mathbf{T}(= \mathbf{T}_d - \mathbf{T})$ to its enantiomeric skeleton, $\widetilde{\sigma}\mathbf{T}(= \mathbf{T}_{\widetilde{\sigma}} - \mathbf{T})$ to its *RS*-diastereomeric skeleton, and $\widehat{I}\mathbf{T}(= \mathbf{T}_{\widehat{I}} - \mathbf{T})$ to its holantimeric skeleton. Thereby, a quadruplet of

Table 1 Operations of $\mathbf{T}_{d\widetilde{\sigma}\widehat{I}}$ and Coset Representation of $\mathbf{T}_{d\widetilde{\sigma}\widehat{I}}(/\mathbf{C}_{3v\widetilde{\sigma}\widehat{I}})$ versus Operations of $\mathbf{O}_h$ and Coset Representation of $\mathbf{O}_h(/\mathbf{D}_{3d})$

operation $g \in \mathbf{O}_h$	operation $g \in \mathbf{T}_{d\widetilde{\sigma}\widehat{I}}$	$\mathbf{O}_h(/\mathbf{D}_{3d})$ or $\mathbf{T}_{d\widetilde{\sigma}\widehat{I}}(/\mathbf{C}_{3v\widetilde{\sigma}\widehat{I}})$ (product of cycles)	operation $g \in \mathbf{O}_h$	operation $g \in \mathbf{T}_{d\widetilde{\sigma}\widehat{I}}$	$\mathbf{O}_h(/\mathbf{D}_{3d})$ or $\mathbf{T}_{d\widetilde{\sigma}\widehat{I}}(/\mathbf{C}_{3v\widetilde{\sigma}\widehat{I}})$ (product of cycles)
I	I	(1)(2)(3)(4)	$C'_{2(6)}$	$\widetilde{\sigma}_{d(1)}$	(1)(2 4)(3)
$C_{2(1)}$	$C_{2(1)}$	(1 2)(3 4)	$C'_{2(1)}$	$\widetilde{\sigma}_{d(6)}$	(1 3)(2)(4)
$C_{2(2)}$	$C_{2(2)}$	(1 4)(2 3)	$C'_{2(4)}$	$\widetilde{\sigma}_{d(5)}$	(1 4)(2)(3)
$C_{2(3)}$	$C_{2(3)}$	(1 3)(2 4)	$C'_{2(2)}$	$\widetilde{\sigma}_{d(2)}$	(1)(2)(3 4)
$C_{3(1)}$	$C_{3(1)}$	(1)(2 3 4)	$C'_{2(5)}$	$\widetilde{\sigma}_{d(3)}$	(1)(2 3)(4)
$C_{3(3)}$	$C_{3(3)}$	(1 3 4)(3)	$C'_{2(3)}$	$\widetilde{\sigma}_{d(4)}$	(1 2)(3)(4)
$C_{3(2)}$	$C_{3(2)}$	(1 4 3)(2)	$C^3_{4(3)}$	$\widetilde{S}_{4(3)}$	(1 2 3 4)
$C_{3(4)}$	$C_{3(4)}$	(1 3 2)(4)	$C_{4(3)}$	$\widetilde{S}^3_{4(3)}$	(1 4 3 2)
$C^2_{3(1)}$	$C^2_{3(1)}$	(1)(2 4 3)	$C^3_{4(1)}$	$\widetilde{S}^3_{4(1)}$	(1 4 2 3)
$C^2_{3(4)}$	$C^2_{3(4)}$	(1 2 3)(4)	$C_{4(1)}$	$\widetilde{S}_{4(1)}$	(1 3 2 4)
$C^2_{3(3)}$	$C^2_{3(3)}$	(1 4 2)(3)	$C_{4(2)}$	$\widetilde{S}^3_{4(2)}$	(1 2 4 3)
$C^2_{3(2)}$	$C^2_{3(2)}$	(1 3 4)(2)	$C^3_{4(2)}$	$\widetilde{S}_{4(2)}$	(1 3 4 2)
$\sigma_{d(1)}$	$\sigma_{d(1)}$	$\overline{(1)(2\,4)(3)}$	i	$\widehat{I}$	$\overline{(1)(2)(3)(4)}$
$\sigma_{d(6)}$	$\sigma_{d(6)}$	$\overline{(1\,3)(2)(4)}$	$\sigma_{h(3)}$	$\widehat{C}_{2(1)}$	$\overline{(1\,2)(3\,4)}$
$\sigma_{d(2)}$	$\sigma_{d(2)}$	$\overline{(1)(2)(3\,4)}$	$\sigma_{h(2)}$	$\widehat{C}_{2(2)}$	$\overline{(1\,4)(2\,3)}$
$\sigma_{d(4)}$	$\sigma_{d(4)}$	$\overline{(1\,2)(3)(4)}$	$\sigma_{h(1)}$	$\widehat{C}_{2(3)}$	$\overline{(1\,3)(2\,4)}$
$\sigma_{d(3)}$	$\sigma_{d(3)}$	$\overline{(1)(2\,3)(4)}$	$S^5_{6(1)}$	$\widehat{C}_{3(1)}$	$\overline{(1)(2\,3\,4)}$
$\sigma_{d(5)}$	$\sigma_{d(5)}$	$\overline{(1\,4)(2)(3)}$	$S^5_{6(3)}$	$\widehat{C}_{3(3)}$	$\overline{(1\,4\,2)(3)}$
$S_{4(3)}$	$S_{4(3)}$	$\overline{(1\,2\,3\,4)}$	$S^5_{6(2)}$	$\widehat{C}_{3(2)}$	$\overline{(1\,4\,3)(2)}$
$S^3_{4(3)}$	$S^3_{4(3)}$	$\overline{(1\,4\,3\,2)}$	$S^5_{6(4)}$	$\widehat{C}_{3(4)}$	$\overline{(1\,2\,3)(4)}$
$S_{4(1)}$	$S_{4(1)}$	$\overline{(1\,4\,2\,3)}$	$S_{6(1)}$	$\widehat{C}^2_{3(1)}$	$\overline{(1)(2\,4\,3)}$
$S^3_{4(1)}$	$S^3_{4(1)}$	$\overline{(1\,3\,2\,4)}$	$S_{6(4)}$	$\widehat{C}_{3(4)^2}$	$\overline{(1\,3\,2)(4)}$
$S^3_{4(2)}$	$S^3_{4(2)}$	$\overline{(1\,2\,4\,3)}$	$S_{6(3)}$	$\widehat{C}^2_{3(3)}$	$\overline{(1\,2\,4)(3)}$
$S_{4(2)}$	$S_{4(2)}$	$\overline{(1\,3\,4\,2)}$	$S_{6(2)}$	$\widehat{C}^2_{3(2)}$	$\overline{(1\,3\,4)(2)}$

RS-stereoisomers is selected as shown in Fig. 2a, where an appropriate representative is selected according to each coset of Eq. 1, i.e.,

$$\begin{aligned}
&\mathbf{1} \quad \text{for} \quad I \quad (\in \mathbf{T}) && \sim (1)(2)(3)(4),\\
&\overline{\mathbf{1}} \quad \text{for} \quad \sigma_{d(1)} (\in \sigma\mathbf{T} = \mathbf{T}_d - \mathbf{T}) && \sim \overline{(1)(2\,4)(3)},\\
&\mathbf{3} \quad \text{for} \quad \widetilde{\sigma}_{d(1)} \quad (\in \widetilde{\sigma}\mathbf{T} = \mathbf{T}_{\widetilde{\sigma}} - \mathbf{T}) && \sim (1)(2\,4)(3), \quad \text{and}\\
&\overline{\mathbf{3}} \quad \text{for} \quad \widehat{I} \quad (\in \widehat{I}\mathbf{T} = \mathbf{T}_{\widehat{I}} - \mathbf{T}) && \sim \overline{(1)(2)(3)(4)}.
\end{aligned}$$

The resulting diagram (Fig. 2a) is here called a *reference stereoisogram*. Strictly speaking, each skeleton collected in Fig. 2a corresponds to a representative of the corresponding coset, i.e., I ($\in \mathbf{T}$) for $\mathbf{1}$, $\sigma_{d(1)}$ ($\in \sigma\mathbf{T} = \mathbf{T}_d - \mathbf{T}$) for $\overline{\mathbf{1}}$, $\widetilde{\sigma}_{d(1)}$ ($\in \widetilde{\sigma}\mathbf{T} = \mathbf{T}_{\widetilde{\sigma}} - \mathbf{T}$) for $\mathbf{3}$, $\widehat{I}$ ($\in \widehat{I}\mathbf{T} = \mathbf{T}_{\widehat{I}} - \mathbf{T}$) for $\overline{\mathbf{3}}$. It should be noted that each representative

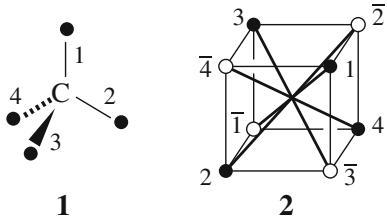

Fig. 1 A reference tetrahedral skeleton **1** and a reference cubic skeleton **2**

skeleton (**1**, $\overline{\mathbf{1}}$, **3**, or $\overline{\mathbf{3}}$) is converted into its homomer under the action of **T**, where the mode of numbering is altered according to **T** so as to result in the numbering due to the respective coset.

The operations of the $\mathbf{T}_d$ collected in the **A**- and **B**-part of Table 1 correspond to respective products of cycles, which are contained in the coset representation $\mathbf{T}_d(/\mathbf{C}_{3v})$ [16]. The products of cycles corresponding to the operations collected in the **C**- and **D**-parts have been originally assigned by taking account of the correspondence between $\sigma\mathbf{T}$ and $\widetilde{\sigma}\mathbf{T}$ or between **T** and $\widehat{I}\mathbf{T}$, where an overline is attached or not [e.g., (1)(2)(3)(4) vs. $\overline{(1)(2)(3)(4)}$ and $\overline{(1)(2\,4)(3)}$ vs. (1)(2 4)(3)] to each product of cycles and a tilde (or hat) accent is attached or not to each operation [e.g., I vs. $\widehat{I}$ and $\sigma_{d(1)}$ vs. $\widetilde{\sigma}_{d(1)}$]. One of the main tasks of the present article to redefine the products of cycles as the elements of the coset representation $\mathbf{T}_{d\widetilde{\sigma}\widehat{I}}(/\mathbf{C}_{3v\widetilde{\sigma}\widehat{I}})$.

To demonstrate the correspondence between $\mathbf{T}_d$ and $\mathbf{O}_h$, let us next examine the cubic skeleton **2** (Fig. 1), where we focus our attention on its four diagonals. The four diagonals of **2** constructs an orbit governed by the coset representation $\mathbf{O}_h(/\mathbf{D}_{3d})$ of degree 4. The $\mathbf{O}_h(/\mathbf{D}_{3d})$-orbit is restricted to $\mathbf{T}_d$ in accord with the subduction of the coset representation:

$$\mathbf{O}_h(/\mathbf{D}_{3d}) \downarrow \mathbf{T}_d = \mathbf{T}_d(/\mathbf{C}_{3v}). \tag{10}$$

The $\mathbf{O}_h(/\mathbf{D}_{3d})$-orbit of the four diagonals of **2** is not separated under this subduction so as to retain one orbit governed by the coset representation $\mathbf{T}_d(/\mathbf{C}_{3v})$.

On the other hand, the eight vertices of **2** is governed by the coset representation of degree 8, i.e., $\mathbf{O}_h(/\mathbf{C}_{3v})$, which is reduced to $\mathbf{T}_d$ according to the following subduction:

$$\mathbf{O}_h(/\mathbf{C}_{3v}) \downarrow \mathbf{T}_d = 2\mathbf{T}_d(/\mathbf{C}_{3v}), \tag{11}$$

where the eight vertices are separated into two $\mathbf{T}_d(/\mathbf{C}_{3v})$-orbits, as designated by solid circles and open circles.

To discuss Eq. 10 (for the four diagonals) and Eq. 11 (for the eight vertices) comprehensively, the eight vertices are numbered from 1 to 4 and from $\overline{1}$ to $\overline{4}$, where the two terminal vertices of each diagonal are designated by a number and its overlined counterpart, as shown in **2**. When the four vertices marked by a solid circle in **2** are considered to correspond to the four vertices of **1**, the reference stereoisogram shown in Fig. 2a can be converted into the reference stereoisogram shown in Fig. 2b.

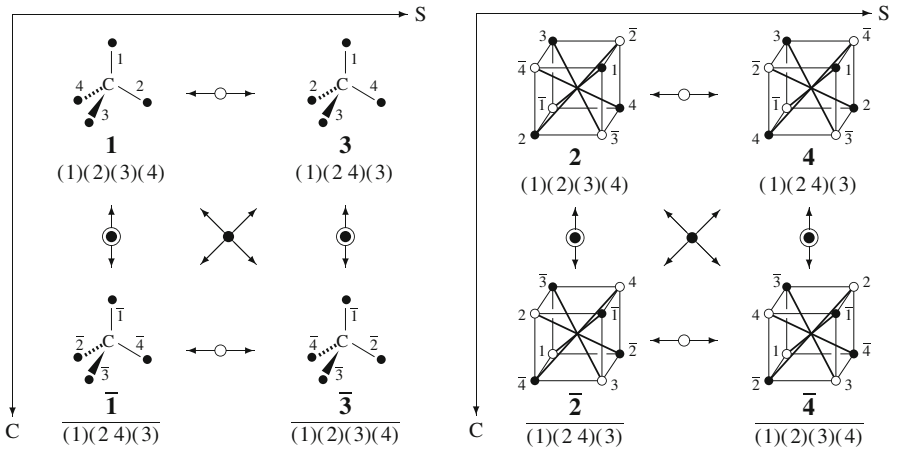

(a) Stereoisogram for a tetrahedral skeleton **(b)** Stereoisogram for a cubic skeleton

Fig. 2 Reference stereoisograms for a tetrahedral skeleton (**a**) and for a cubic skeleton (**b**)

3 Point groups isomorphic to *RS*-stereoisomeric groups

3.1 Operations of $\mathbf{T}_{d\tilde{\sigma}\hat{I}}$ and those of $\mathbf{O}_h$

According to the definition of $\mathbf{T}_{d\tilde{\sigma}\hat{I}}$, the $\mathbf{T}_d$-part of $\mathbf{T}_{d\tilde{\sigma}\hat{I}}$ is isomorphic to (the same as) the $\mathbf{T}_d$-part of $\mathbf{O}_h$. Let us first examine $\sigma_{d(1)}(\sim \overline{(1)(2\,4)(3)})$, which is an element of $\mathbf{T}_d - \mathbf{T}\,(\subset \mathbf{T}_{d\tilde{\sigma}\hat{I}}$ or $\subset \mathbf{O}_h)$. As found in Fig. 3a, the operation $\sigma_{d(1)}$ converts **5** into **6** under the action of $\mathbf{T}_{d\tilde{\sigma}\hat{I}}$ or $\mathbf{O}_h$, where the operation $\sigma_{d(1)}$ requires no bond cleavage nor distortion. This means that this conversion retains the framework of the tetrahedral skeleton (within the cubic skeleton). Note that any operation of a point group for a skeleton retains the framework of the skeleton at issue.

As illustrated in Fig. 3b, the operation $\widetilde{\sigma}_{d(1)}\,(\sim (1)(2\,4)(3))$, which is an element of $\mathbf{T}_{\tilde{\sigma}} - \mathbf{T}\,(\subset \mathbf{T}_{d\tilde{\sigma}\hat{I}})$, requires bond cleavage or distortion (e.g., pseudo-rotation) during the conversion of **5** into **7**. This means that this conversion does not retain the framework of the tetrahedral skeleton (within the cubic skeleton), if we take account of the *RS*-stereoisomeric group $\mathbf{T}_{d\tilde{\sigma}\hat{I}}$.

On the other hand, the operation $\mathrm{C}'_{2(1)}\,(\sim (1)(2\,4)(3)$ for the four diagonals), which is an element of $\mathbf{O} - \mathbf{T}\,(\subset \mathbf{O}_h)$, converts **5** into **8**, where the operation $\mathrm{C}'_{2(1)}$ requires no bond cleavage. This means that this conversion retains the framework of the tetrahedral skeleton (within the cubic skeleton), if we take account of the point group $\mathbf{O}_h$.

To clarify the isomorphism between $\mathbf{T}_{d\tilde{\sigma}\hat{I}}$ and $\mathbf{O}_h$, the resulting skeletons **7** (with bond cleavage or distortion) and **8** (without distortion) should be recognized to be dual. The duality between **7** and **8** can be accomplished by considering a duality operation in which each solid circle and each open circle are exchanged and each number and its overlined counterpart are exchanged. Thereby, the correspondence between $\widetilde{\sigma}_{d(1)}\,(\sim (1)(2\,4)(3))$ and $\mathrm{C}'_{2(1)}\,(\sim (1)(2\,4)(3))$ is recognized to be a pair of dual

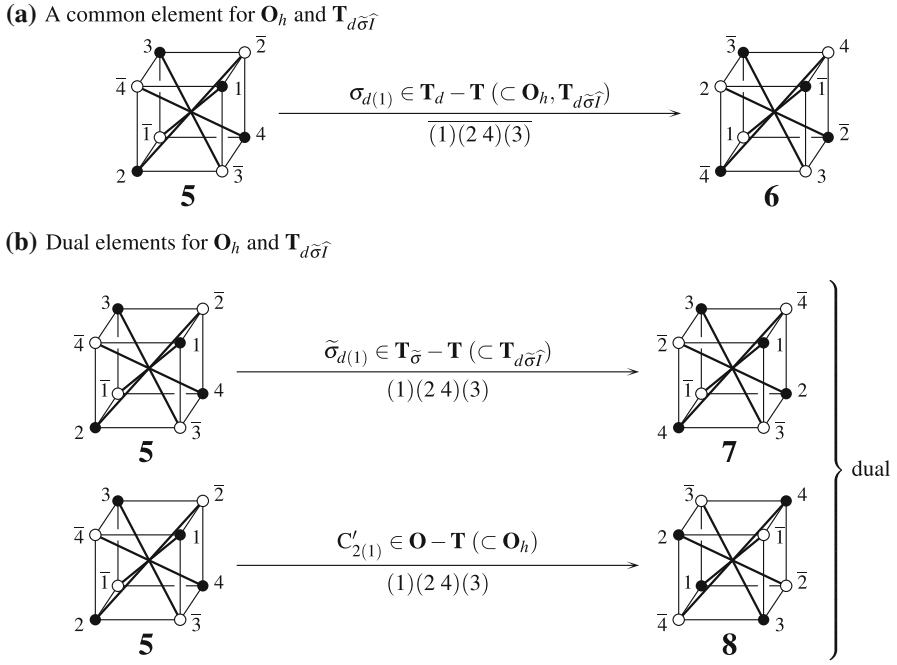

Fig. 3 Correspondence between elements of point groups and those *RS*-stereoisomeric groups. **a** An element $\sigma_{d(1)}$ is contained in $\mathbf{T}_d - \mathbf{T}$, which is a subgroup for $\mathbf{O}_h$ and $\mathbf{T}_{d\tilde{\sigma}\hat{I}}$. **b** An element $\tilde{\sigma}_{d(1)}$ is contained in $\mathbf{T}_{\tilde{\sigma}} - \mathbf{T}$, which is a subgroup of an *RS*-stereoisomeric group $\mathbf{T}_{d\tilde{\sigma}\hat{I}}$; while $C'_{2(1)}$ is contained in $\mathbf{O} - \mathbf{T}$, which is a subgroup of a point group $\mathbf{O}_h$

elements to assure the isomorphism between $\mathbf{T}_{d\tilde{\sigma}\hat{I}}$ and $\mathbf{O}_h$, as shown in Fig. 3b. The permutation (1)(2 4)(3) for $\tilde{\sigma}_{d(1)}$ ($\in \mathbf{T}_{d\tilde{\sigma}\hat{I}}$) is apparently identical with the permutation (1)(2 4)(3) for $C'_{2(1)}$ ($\in \mathbf{O}_h$), although their objects (vertices vs. diagonals) are different.

Let us second examine $C_{2(1)}$ ($\sim$ (1 2)(3 4)), which is an operation contained in **T**. Note that **T** is a subgroup of $\mathbf{T}_d$, which is a common subgroup of $\mathbf{T}_{d\tilde{\sigma}\hat{I}}$ or $\mathbf{O}_h$. As found in Fig. 4a, the conversion of **5** into **9** requires no bond cleavage so as to retain the framework of the tetrahedral skeleton (within the cubic skeleton).

As found in Fig. 4b, the operation $\widehat{C}_{2(1)}$ ($\sim \overline{(1\,2)(3\,4)}$), which is contained in $\mathbf{T}_{\hat{I}} - \mathbf{T}\ (\subset \mathbf{T}_{d\tilde{\sigma}\hat{I}})$, converts **5** into **10**, where bond cleavage is necessary in the process of exchanging 1 and $\overline{1}$, etc. (cf. **9** → **10**).

On the other hand, the operation $\sigma_{h(3)}$ ($\sim \overline{(1\,2)(3\,4)}$), which is contained in $\mathbf{T}_h - \mathbf{T}\ (\subset \mathbf{O}_h)$, converts **5** into **11** without bond cleavage.

To clarify the isomorphism between $\mathbf{T}_{d\tilde{\sigma}\hat{I}}$ and $\mathbf{O}_h$, **10** and **11** are recognized to be dual in terms of a duality operation in which each solid circle and each open circle are exchanged and each number and its overlined counterpart are exchanged. It follows that $\widehat{C}_{2(1)}$ ($\sim \overline{(1\,2)(3\,4)}$) and $\sigma_{h(3)}$ ($\sim \overline{(1\,2)(3\,4)}$) are recognized to be dual elements so as to assure the isomorphism between $\mathbf{T}_{d\tilde{\sigma}\hat{I}}$ and $\mathbf{O}_h$, as shown in in Fig. 4b. The permutation $\overline{(1\,2)(3\,4)}$ for $\widehat{C}_{2(1)}$ ($\in \mathbf{T}_{d\tilde{\sigma}\hat{I}}$) and the permutation $\overline{(1\,2)(3\,4)}$ for

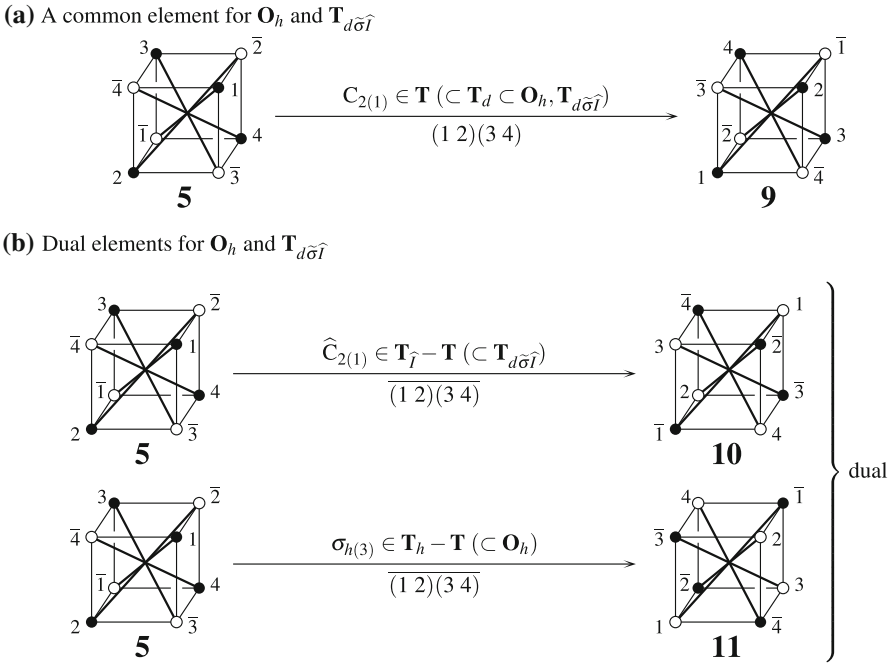

Fig. 4 Correspondence between elements of point groups and those *RS*-stereoisomeric groups. **a** An element $C_{2(1)}$ is contained in **T**, which is a subgroup for $\mathbf{O}_h$ and $\mathbf{T}_{d\tilde{\sigma}\hat{I}}$. **b** An element $\hat{C}_{2(1)}$ is contained in $\mathbf{T}_{\hat{I}} - \mathbf{T}$, which is a subgroup of an *RS*-stereoisomeric group $\mathbf{T}_{d\tilde{\sigma}\hat{I}}$, while $\sigma_{h(3)}$ is contained in $\mathbf{T}_h - \mathbf{T}$, which is a subgroup of a point group $\mathbf{O}_h$

$\sigma_{h(3)}$ ($\in \mathbf{O}_h$) are apparently identical with each other, although their objects (vertices vs. diagonals) are different.

Let us third examine the identity element I ($\sim$ (1)(2)(3)(4)), which is an operation contained in **T**. Note that **T** is a subgroup of $\mathbf{T}_d$, which is a common subgroup of $\mathbf{T}_{d\tilde{\sigma}\hat{I}}$ or $\mathbf{O}_h$. As found in Fig. 5a, the identity conversion of **5** into **5** requires no bond cleavage so as to retain the framework of the tetrahedral skeleton (within the cubic skeleton).

As found in Fig. 5b, the operation $\hat{I}$ ($\sim \overline{(1)(2)(3)(4)}$), which is contained in $\mathbf{T}_{\hat{I}} - \mathbf{T}$ ($\subset \mathbf{T}_{d\tilde{\sigma}\hat{I}}$) converts **5** into **12**, where bond cleavage is necessary in the process of exchanging 1 and $\overline{1}$ and so on. The exchange between 1 and $\overline{1}$ etc. serves as a basis of the exchange between a proligand (e.g., p) and a counterpart proligand of the opposite chirality (e.g., $\overline{\text{p}}$), which requires bond cleavage.

On the other hand, the inversion operation i ($\sim \overline{(1)(2)(3)(4)}$), which is contained in $\mathbf{T}_h - \mathbf{T}$ ($\subset \mathbf{O}_h$), converts **5** into **13** without bond cleavage.

To clarify the isomorphism between $\mathbf{T}_{d\tilde{\sigma}\hat{I}}$ and $\mathbf{O}_h$, **12** and **13** are recognized to be dual in terms of a duality operation in which each solid circle and each open circle are exchanged and each number and its overlined counterpart are exchanged. It follows that $\hat{I}$ ($\sim \overline{(1)(2)(3)(4)}$) and i ($\sim \overline{(1)(2)(3)(4)}$) are recognized to be dual elements so as to assure the isomorphism between $\mathbf{T}_{d\tilde{\sigma}\hat{I}}$ and $\mathbf{O}_h$, as shown in in Fig. 5b. The

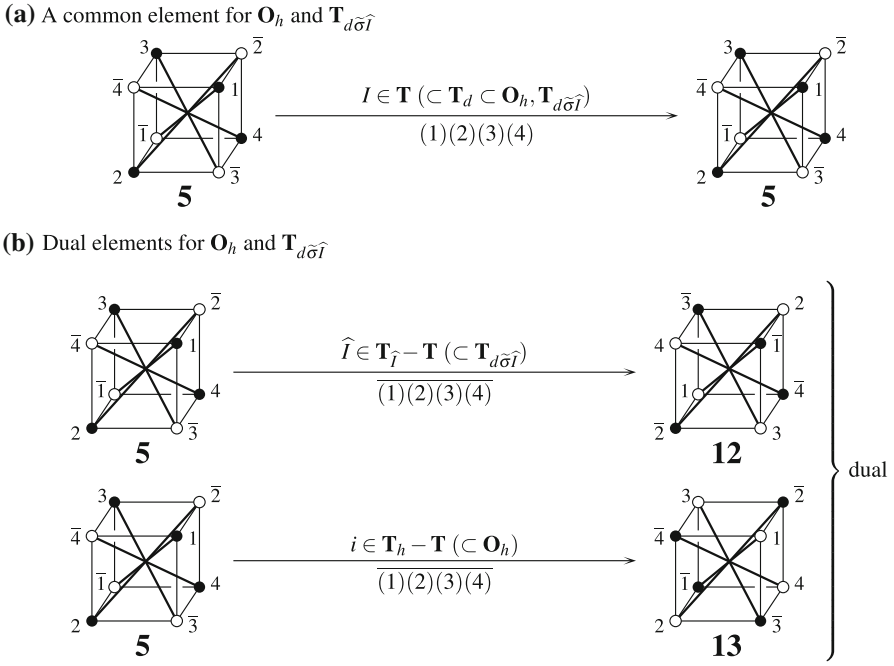

Fig. 5 Correspondence between elements of point groups and those *RS*-stereoisomeric groups. **a** An element $C_{2(1)}$ is contained in $\mathbf{T}$, which is a subgroup for $\mathbf{O}_h$ and $\mathbf{T}_{d\tilde{\sigma}\hat{I}}$. **b** An element $\widehat{C}_{2(1)}$ is contained in $\mathbf{T}_{\hat{I}} - \mathbf{T}$, which is a subgroup of an *RS*-stereoisomeric group $\mathbf{T}_{d\tilde{\sigma}\hat{I}}$, while $\sigma_{h(3)}$ is contained in $\mathbf{T}_h - \mathbf{T}$, which is a subgroup of a point group $\mathbf{O}_h$

permutation $\overline{(1)(2)(3)(4)}$ for $\hat{I}\ (\in \mathbf{T}_{d\tilde{\sigma}\hat{I}})$ and the permutation $\overline{(1)(2)(3)(4)}$ for the inversion operation $i\ (\in \mathbf{O}_h)$ are apparently identical with each other, although their objects (vertices vs. diagonals) are different.

Similar examinations are conducted with respect to the remaining operations of $\mathbf{T}_{d\tilde{\sigma}\hat{I}}$ and those of the point group $\mathbf{O}_h$. The resulting correspondence is summarized in Table 1. The subgroups of $\mathbf{T}_{d\tilde{\sigma}\hat{I}}$ shown by Eqs. 5–9 correspond to the following subgroups of $\mathbf{O}_h$ ($\mathbf{A}$, $\mathbf{B}$, $\mathbf{C}$, $\mathbf{D}$ are gray letters):

$$\mathbf{O}_h = \{\mathbf{A}, \mathbf{B}, \mathbf{C}, \mathbf{D}\} \tag{12}$$

$$\mathbf{T}_d = \{\mathbf{A}, \mathbf{B}\} \tag{13}$$

$$\mathbf{O} = \{\mathbf{A}, \mathbf{C}\} \tag{14}$$

$$\mathbf{T}_h = \{\mathbf{A}, \mathbf{D}\} \tag{15}$$

$$\mathbf{T} = \{\mathbf{A}\}. \tag{16}$$

The comparison between Eqs. 5–9 and Eqs. 12–16 results in the following set of isomorphism: $\mathbf{O}_h \cong \mathbf{T}_{d\tilde{\sigma}\hat{I}}$, $\mathbf{T}_d = \mathbf{T}_d$ (identical), $\mathbf{O} \cong \mathbf{T}_{\tilde{\sigma}}$, and $\mathbf{T}_h \cong \mathbf{T}_{\hat{I}}$, and $\mathbf{T} = \mathbf{T}$ (identical). It follows that Eqs. 1–4 for the *RS*-stereoisomeric group $\mathbf{T}_{d\tilde{\sigma}\hat{I}}$ correspond respectively to the coset decompositions for the point group $\mathbf{O}_h$:

$$\mathbf{O}_h = \mathbf{T} + \sigma_{d(1)}\mathbf{T} + C'_{2(6)}\mathbf{T} + i\mathbf{T} \tag{17}$$

$$\mathbf{T}_d = \mathbf{T} + \sigma_{d(1)}\mathbf{T} \tag{18}$$

$$\mathbf{O} = \mathbf{T} + C'_{2(6)}\mathbf{T} \tag{19}$$

$$\mathbf{T}_h = \mathbf{T} + i\mathbf{T} \tag{20}$$

3.2 Symmetry elements of $\mathbf{T}_{d\widetilde{\sigma}\widehat{I}}$ and those of $\mathbf{O}_h$

Symmetry elements of the point group $\mathbf{O}_h$ are shown in Fig. 6, which is a modification of Fig. 2.2 of [46]. Note that the diagram of the inversion center is omitted and that the numbering of the vertices are changed from the original numbering [46]. The top row depicts rotation or rotoreflection axes: **14a**–**14c**; and the bottom row depicts mirror planes: **14d**–**14g**. For example, the $C_{4(3)}$-axis in **14a** generates the operations $C_{4(3)}$, $C_{2(3)}$ $(= C^2_{4(3)})$, and $C^3_{4(3)}$, where it implies the presence of the $\mathbf{C}_{2(3)}$-axis. On the other hand, the $S_{4(3)}$-axis in **14a** generates the operations $S_{4(3)}$, $C_{2(3)}$ $(= S^2_{4(3)})$, and $= S^3_{4(3)}$, where it also implies the presence of the $C_{2(3)}$-axis.

As summarized in Table 1, Figs. 3, 4 and 5 provide the correspondence between the operations of the point group $\mathbf{O}_h$ and those of the *RS*-stereoisomeric group $\mathbf{T}_{d\widetilde{\sigma}\widehat{I}}$. Thereby, symmetry elements of the *RS*-stereoisomeric group $\mathbf{T}_{d\widetilde{\sigma}\widehat{I}}$ are obtained as shown in Fig. 7, which corresponds to Fig. 6. The symmetry elements without a tilde or hat accent in Fig. 7 depict rotation or rotoreflection axes, which construct the point group $\mathbf{T}_d$ $(\subset \mathbf{T}_{d\widetilde{\sigma}\widehat{I}})$. The symmetry elements with a tilde or hat accent construct the coset $\mathbf{T}_{d\widetilde{\sigma}\widehat{I}} - \mathbf{T}_d$ (i.e., {**C**, **D**} as gray letters). For example, the $\widetilde{S}_{4(3)}$-axis in

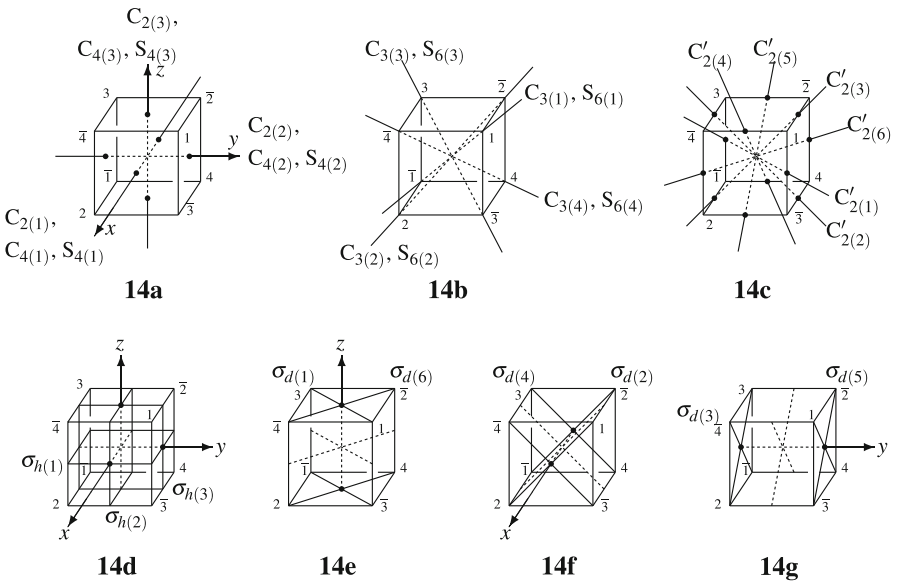

Fig. 6 Symmetry elements of the point group $\mathbf{O}_h$ for characterizing a cubane skeleton [46]. The *top row* depicts rotation or rotoreflection axes: **14a**–**14c**; and the *bottom row* depicts mirror planes: **14d**–**14g**

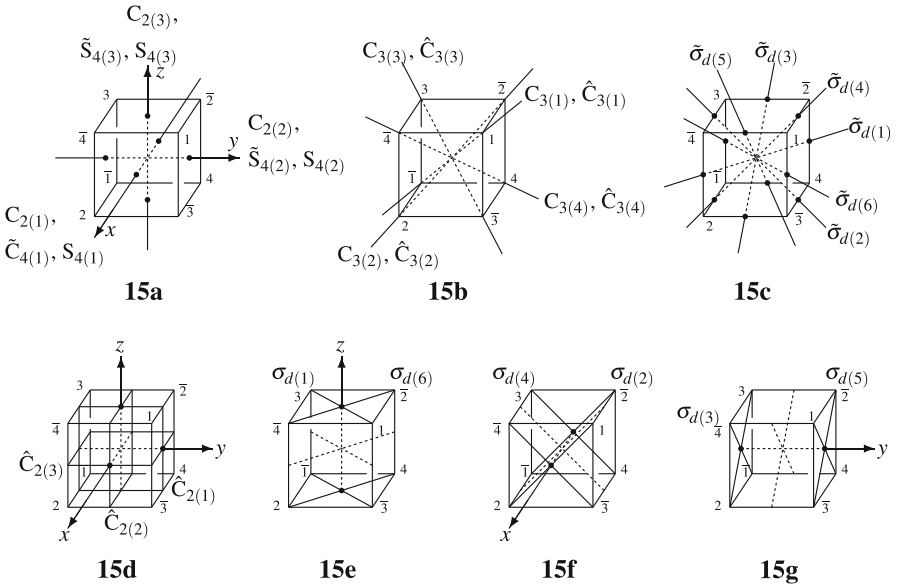

Fig. 7 Symmetry elements of the *RS*-stereoisomeric group $\mathbf{T}_{d\widetilde{\sigma}\widehat{I}}$ for characterizing a cubane skeleton. The symmetry elements without a tilde or hat accent depict rotation or rotoreflection axes, which construct the point group $\mathbf{T}_d$ ($\subset \mathbf{T}_{d\widetilde{\sigma}\widehat{I}}$). The symmetry elements with a tilde or hat accent construct the coset $\mathbf{T}_{d\widetilde{\sigma}\widehat{I}} - \mathbf{T}_d$

15a generates the operations $\widetilde{S}_{4(3)}$, $C_{2(3)}$ $(= \widetilde{S}^2_{4(3)})$, and $\widetilde{S}^3_{4(3)}$, where it implies the presence of the $C_{2(3)}$-axis. On the other hand, the $S_{4(3)}$-axis for the *RS*-stereoisomeric group $\mathbf{T}_{d\widetilde{\sigma}\widehat{I}}$ is identical with the $S_{4(3)}$-axis for the point group $\mathbf{O}_h$, which generates the operations $S_{4(3)}$, $C_{2(3)}(= S^2_{4(3)})$, and $= S^3_{4(3)}$.

3.3 Factor groups derived from $\mathbf{T}_{d\widetilde{\sigma}\widehat{I}}$ and $\mathbf{O}_h$

Because the subgroup $\mathbf{T}$ is a normal subgroup of $\mathbf{T}_{d\widetilde{\sigma}\widehat{I}}$, Eq. 1 provides a factor group:

$$\mathbf{T}_{d\widetilde{\sigma}\widehat{I}}/\mathbf{T} = \{\mathbf{T}, \sigma\mathbf{T}, \widetilde{\sigma}\mathbf{T}, \widehat{I}\mathbf{T}\}. \tag{21}$$

As proved generally [34], a factor group generated from an *RS*-stereoisomeric group is isomorphic to the point group $\mathbf{C}_{2v}$ or the Klein four-group, so that it has five subgroups only, just as the point group $\mathbf{C}_{2v}$ or the Klein four-group has subgroups only. The five subgroups are named Type I–V as follows:

$$\text{Type IV} \quad \{\mathbf{T}, \sigma\mathbf{T}, \widetilde{\sigma}\mathbf{T}, \widehat{I}\mathbf{T}\} \tag{22}$$
$$\text{Type V} \quad \{\mathbf{T}, \sigma\mathbf{T}\} \tag{23}$$
$$\text{Type II} \quad \{\mathbf{T}, \widetilde{\sigma}\mathbf{T}\} \tag{24}$$
$$\text{Type I} \quad \{\mathbf{T}, \widehat{I}\mathbf{T}\} \tag{25}$$
$$\text{Type III} \quad \{\mathbf{T}\} \tag{26}$$

These five types create stereoisograms of five types [34]. They are related to the coset decompositions represented by Eqs. 1–4 or by Eqs. 5–8 (along with Eq. 9).

In a parallel way, Eq. 17 provides another factor group:

$$\mathbf{O}_h/\mathbf{T} = \{\mathbf{T}, \sigma_{d(1)}\mathbf{T}, C'_{2(6)}\mathbf{T}, i\mathbf{T}\} \tag{27}$$

which is isomorphic to the point group $\mathbf{C}_{2v}$ or the Klein four-group. The factor group $\mathbf{O}_h/\mathbf{T}$ has five subgroups only. They are related to the coset decompositions represented by Eqs. 17–20 or by Eqs. 12–15 (along with Eq. 16).

3.4 Subgroups of $\mathbf{T}_{d\tilde{\sigma}\hat{I}}$ and Those of $\mathbf{O}_h$

The point group $\mathbf{O}_h$ has 33 subgroups up to conjugacy, which have been discussed in detail in terms of a non-redundant set of subgroups (SSG) [47]:

$$\begin{aligned}\mathrm{SSG}_{\mathbf{O}_h} = \Big\{ &\overset{1}{\mathbf{C}}_1, \overset{2}{\mathbf{C}}_2, \overset{3}{\mathbf{C}}'_2, \overset{4}{\mathbf{C}}_s, \overset{5}{\mathbf{C}}'_s, \overset{6}{\mathbf{C}}_i, \overset{7}{\mathbf{C}}_3, \overset{8}{\mathbf{C}}_4, \overset{9}{\mathbf{S}}_4, \overset{10}{\mathbf{D}}_2, \overset{11}{\mathbf{D}}'_2, \overset{12}{\mathbf{C}}_{2v}, \overset{13}{\mathbf{C}}'_{2v}, \overset{14}{\mathbf{C}}''_{2v}, \overset{15}{\mathbf{C}}_{2h}, \overset{16}{\mathbf{C}}'_{2h}, \\ &\overset{17}{\mathbf{D}}_3, \overset{18}{\mathbf{C}}_{3v}, \overset{19}{\mathbf{C}}_{3i}, \overset{20}{\mathbf{D}}_4, \overset{21}{\mathbf{C}}_{4v}, \overset{22}{\mathbf{C}}_{4h}, \overset{23}{\mathbf{D}}_{2d}, \overset{24}{\mathbf{D}}'_{2d}, \overset{25}{\mathbf{D}}_{2h}, \overset{26}{\mathbf{D}}'_{2h}, \overset{27}{\mathbf{T}}, \overset{28}{\mathbf{D}}_{3d}, \overset{29}{\mathbf{D}}_{4h}, \\ &\overset{30}{\mathbf{O}}, \overset{31}{\mathbf{T}}_h, \overset{32}{\mathbf{T}}_d, \overset{33}{\mathbf{O}}_h \Big\}\end{aligned} \tag{28}$$

where the subgroups are aligned in the ascending order of their orders. For the convenience of cross reference, sequential numbers from 1 to 33 are attached to the respective subgroups. In accord with Eqs. 17–20 (and the trivial case of $\mathbf{T}$), the subgroups collected in Eq. 28 are categorized to give five categories, as shown in Fig. 8:

1. five subgroups of $\mathbf{T}$,
2. six subgroups of $\mathbf{T}_d$ except those of $\mathbf{T}$,
3. six subgroups of $\mathbf{O}$ except those of $\mathbf{T}$,
4. seven subgroups of $\mathbf{T}_h$ except those of $\mathbf{T}$, and
5. nine subgroups of $\mathbf{O}_h$ except those of $\mathbf{T}$, $\mathbf{T}_d$, $\mathbf{O}$, and $\mathbf{T}_h$.

Because the *RS*-stereoisomeric group $\mathbf{T}_{d\tilde{\sigma}\hat{I}}$ is isomorphic to the point group $\mathbf{O}_h$, there appear 33 subgroups of $\mathbf{T}_{d\tilde{\sigma}\hat{I}}$, which are isomorphic to those of $\mathbf{O}_h$, as summarized in Fig. 8. By referring to the correspondence between the operations of $\mathbf{T}_{d\tilde{\sigma}\hat{I}}$ and those of $\mathbf{O}_h$ (Table 1), the respective subgroups of $\mathbf{T}_{d\tilde{\sigma}\hat{I}}$ are constructed as follows:

1. The five subgroups of the point group $\mathbf{T}$ are also the subgroups of the *RS*-stereoisomeric group $\mathbf{T}_{d\tilde{\sigma}\hat{I}}$. The symbols of the point groups are also used to designate the subgroups of the *RS*-stereoisomeric group. See Fig. 8. These *RS*-stereoisomeric groups are categorized to type III.
2. The six subgroups of $\mathbf{T}_d$ (except those of $\mathbf{T}$) are the subgroups of the *RS*-stereoisomeric group $\mathbf{T}_{d\tilde{\sigma}\hat{I}}$ at the same time. The symbols of the point groups are also used to designate the subgroups of the *RS*-stereoisomeric group except that the symbols $\mathbf{C}'_s$ and $\mathbf{C}'_{2v}$ in $\mathbf{O}_h$ are changed into $\mathbf{C}_s$ and $\mathbf{C}_{2v}$ in $\mathbf{T}_{d\tilde{\sigma}\hat{I}}$ because

$\subset \mathbf{O}_h$ $\subset \mathbf{T}_{d\widetilde{\sigma}\widehat{I}}$ (Type)	Subgroups														
	1	2		7	10							27			
$\mathbf{T}$	$\mathbf{C}_1$	$\mathbf{C}_2$		$\mathbf{C}_3$	$\mathbf{D}_2$							$\mathbf{T}$			
$\mathbf{T}$ (III)	$\mathbf{C}_1$	$\mathbf{C}_2$		$\mathbf{C}_3$	$\mathbf{D}_2$							$\mathbf{T}$			
		5			9	13	18	23						32	
$\mathbf{T}_d$		$\mathbf{C}'_s$			$\mathbf{S}_4$	$\mathbf{C}'_{2v}$	$\mathbf{C}_{3v}$	$\mathbf{D}_{2d}$						$\mathbf{T}_d$	
$\mathbf{T}_d$ (V)		$\mathbf{C}_s$			$\mathbf{S}_4$	$\mathbf{C}_{2v}$	$\mathbf{C}_{3v}$	$\mathbf{D}_{2d}$						$\mathbf{T}_d$	
		3			8	11	17	20						30	
$\mathbf{O}$		$\mathbf{C}'_2$			$\mathbf{C}_4$	$\mathbf{D}'_2$	$\mathbf{D}_3$	$\mathbf{D}_4$						$\mathbf{O}$	
$\mathbf{T}_{\widetilde{\sigma}}$ (II)		$\mathbf{C}_{\widetilde{\sigma}}$			$\mathbf{S}_{\widetilde{4}}$	$\mathbf{C}_{2\widetilde{\sigma}}$	$\mathbf{C}_{3\widetilde{\sigma}}$	$\mathbf{D}_{2\widetilde{\sigma}}$						$\mathbf{T}_{\widetilde{\sigma}}$	
		4	6		12	15	19	25						31	
$\mathbf{T}_h$		$\mathbf{C}_s$	$\mathbf{C}_i$		$\mathbf{C}_{2v}$	$\mathbf{C}_{2h}$	$\mathbf{C}_{3i}$	$\mathbf{D}_{2h}$						$\mathbf{T}_h$	
$\mathbf{T}_{\widehat{I}}$ (I)		$\mathbf{C}_{\widehat{\sigma}}$	$\mathbf{C}_{\widehat{I}}$		$\mathbf{C}_{2\widehat{\sigma}}$	$\mathbf{C}_{2\widehat{I}}$	$\mathbf{C}_{3\widehat{I}}$	$\mathbf{D}_{2\widehat{I}}$						$\mathbf{T}_{\widehat{I}}$	
					14	16		21	22	24	26	28	29		33
$\mathbf{O}_h$					$\mathbf{C}''_{2v}$	$\mathbf{C}'_{2h}$		$\mathbf{C}_{4v}$	$\mathbf{C}_{4h}$	$\mathbf{D}'_{2d}$	$\mathbf{D}'_{2h}$	$\mathbf{D}_{3d}$	$\mathbf{D}_{4h}$		$\mathbf{O}_h$
$\mathbf{T}_{d\widetilde{\sigma}\widehat{I}}$ (IV)					$\mathbf{C}_{s\widetilde{\sigma}\widehat{\sigma}}$	$\mathbf{C}_{s\widetilde{\sigma}\widehat{I}}$		$\mathbf{S}_{\widetilde{4}\widehat{\sigma}}$	$\mathbf{S}_{\widetilde{4}\widehat{I}}$	$\mathbf{S}_{4\widetilde{\sigma}\widehat{\sigma}}$	$\mathbf{C}_{2v\widetilde{\sigma}\widehat{I}}$	$\mathbf{C}_{3v\widetilde{\sigma}\widehat{I}}$	$\mathbf{D}_{2d\widetilde{\sigma}\widehat{I}}$		$\mathbf{T}_{d\widetilde{\sigma}\widehat{I}}$
order	1	2		3	4		6	8				12	16	24	48

Fig. 8 Subgroups of the point group $\mathbf{O}_h$ and the corresponding isomorphic subgroups of the *RS*-stereoisomeric group $\mathbf{T}_{d\widetilde{\sigma}\widehat{I}}$. For the convenience of cross reference to Eqs. 28 and 51, sequential numbers from 1 to 33 are attached to the respective subgroups. The symbols for the subgroups of $\mathbf{T}_d$ are essentially common in both of the two isomorphic series. The symbol for each subgroup of $\mathbf{T}_{\widetilde{\sigma}}$ (II) contains a tilde accent. The symbol for each subgroup of $\mathbf{T}_{\widehat{I}}$ (I) contains a hat accent. The symbol for each subgroup of $\mathbf{T}_{d\widetilde{\sigma}\widehat{I}}$ (IV) contains both a tilde and a hat accent

of no confusion. See Fig. 8. These *RS*-stereoisomeric groups are categorized to type V.

3. The six subgroups of $\mathbf{O}$ (except those of $\mathbf{T}$) correspond to the following subgroups of $\mathbf{T}_{\widetilde{\sigma}}$ $(-\mathbf{T})$.

$$\mathbf{C}_{\widetilde{\sigma}} = \{I, \widetilde{\sigma}_{d(1)}\} \qquad (\supset \mathbf{C}_1) \tag{29}$$

$$\mathbf{S}_{\widetilde{4}} = \{I, \widetilde{S}_{4(3)}, C_{2(3)}, \widetilde{S}^3_{4(3)}\} \qquad (\supset \mathbf{C}_2) \tag{30}$$

$$\mathbf{C}_{2\widetilde{\sigma}} = \{I, C_{2(3)}, \widetilde{\sigma}_{d(1)}, \widetilde{\sigma}_{d(6)}\} \qquad (\supset \mathbf{C}_2) \tag{31}$$

$$\mathbf{C}_{3\widetilde{\sigma}} = \{I, C_{3(1)}, C^2_{3(1)}, \widetilde{\sigma}_{d(1)}, \widetilde{\sigma}_{d(2)}, \widetilde{\sigma}_{d(3)}\} \qquad (\supset \mathbf{C}_3) \tag{32}$$

$$\mathbf{D}_{2\widetilde{\sigma}} = \{I, C_{2(1)}, C_{2(2)}, C_{2(3)}, \widetilde{\sigma}_{d(1)}, \widetilde{\sigma}_{d(6)}, \widetilde{S}_{4(3)}, \widetilde{S}^3_{4(3)}\} \qquad (\supset \mathbf{D}_2) \tag{33}$$

$$\mathbf{T}_{\widetilde{\sigma}} = \{\mathbf{A}, \mathbf{C}\} \qquad (\supset \mathbf{T}) \qquad (\text{cf. Eq. 7}) \tag{34}$$

The symbols of the subgroups are selected by designating a common subgroup to $\mathbf{T}_d$ (denoted in a pair of parentheses) which is attached by a suffix to refer to an uncommon operation. Each of the symbols contains a tilde accent in its suffix. For example, the symbol $\mathbf{C}_{2\widetilde{\sigma}}$ stems from the largest subgroup $\mathbf{C}_2$ (as a common subgroup to $\mathbf{T}_d$) and from an uncommon operation $\widetilde{\sigma}_{d(1)}$. The symbol $\mathbf{S}_{\widetilde{4}}$ is adopted for the purpose of avoiding the confusion with $\mathbf{C}_{2\widetilde{\sigma}}$. These *RS*-stereoisomeric groups are categorized to type II.

4. The seven subgroups of $\mathbf{T}_h$ (except those of $\mathbf{T}$) correspond to the following subgroups of $\mathbf{T}_{\widehat{I}}\,(-\mathbf{T})$.

$$\mathbf{C}_{\widehat{\sigma}} = \{I, \widehat{C}_{2(3)}\} \quad (\supset \mathbf{C}_1) \tag{35}$$

$$\mathbf{C}_{\widehat{I}} = \{I, \widehat{I}\} \quad (\supset \mathbf{C}_1) \tag{36}$$

$$\mathbf{C}_{2\widehat{\sigma}} = \{I, C_{2(3)}, \widehat{C}_{2(1)}, \widehat{C}_{2(2)}\} \quad (\supset \mathbf{C}_2) \tag{37}$$

$$\mathbf{C}_{2\widehat{I}} = \{I, C_{2(3)}, \widehat{C}_{2(3)}, \widehat{I}\} \quad (\supset \mathbf{C}_2) \tag{38}$$

$$\mathbf{C}_{3\widehat{I}} = \{I, C_{3(1)}, C^2_{3(1)}, \widehat{I}, \widehat{C}_{3(1)}, \widehat{C}^2_{3(1)}\} \quad (\supset \mathbf{C}_3) \tag{39}$$

$$\mathbf{D}_{2\widehat{I}} = \{I, C_{2(1)}, C_{2(2)}, C_{2(3)}, \widehat{I}, \widehat{C}_{2(1)}, \widehat{C}_{2(2)}, \widehat{C}_{2(3)}\} \quad (\supset \mathbf{D}_2) \tag{40}$$

$$\mathbf{T}_{\widehat{I}} = \{\mathbf{A}, \mathbf{D}\} \quad (\supset \mathbf{T}) \quad \text{(cf. Eq. 9)} \tag{41}$$

The suffix $\widehat{\sigma}$ is used to refer to $\widehat{C}_{2(1)}$ and so on. The names of the subgroups are characterized by the symbols with a hat accent. These *RS*-stereoisomeric groups are categorized to type I.

5. The nine subgroups of $\mathbf{O}_h$ (except those of $\mathbf{T}$, $\mathbf{T}_d$, $\mathbf{O}$, and $\mathbf{T}_h$) correspond to the following subgroups of $\mathbf{T}_{d\widetilde{\sigma}\widehat{I}}$.

$$\mathbf{C}_{s\widetilde{\sigma}\widehat{\sigma}} = \{I, \widetilde{\sigma}_{d(1)}, \widehat{C}_{2(3)}, \sigma_{d(6)}\} \quad (\supset \mathbf{C}_s) \tag{42}$$

$$\mathbf{C}_{s\widetilde{\sigma}\widehat{I}} = \{I, \widetilde{\sigma}_{d(1)}, \widehat{I}, \sigma_{d(1)}\} \quad (\supset \mathbf{C}_s) \tag{43}$$

$$\mathbf{S}_{\widetilde{4}\widehat{\sigma}} = \{I, \widetilde{S}_{4(3)}, C_{2(3)}, \widetilde{S}^3_{4(3)}, \widehat{C}_{2(1)}, \widehat{C}_{2(2)}, \sigma_{d(1)}, \sigma_{d(6)}\} \quad (\supset \mathbf{S}_{\widetilde{4}}, \mathbf{C}_{2v}) \tag{44}$$

$$\mathbf{S}_{\widetilde{4}\widehat{I}} = \{I, \widetilde{S}_{4(3)}, C_{2(3)}, \widetilde{S}^3_{4(3)}, \widehat{I}, \widehat{C}_{2(3)}, S_{4(3)}, S^3_{4(3)}\} \quad (\supset \mathbf{S}_{\widetilde{4}}, \mathbf{S}_4) \tag{45}$$

$$\mathbf{S}_{4\widetilde{\sigma}\widehat{\sigma}} = \{I, C_{2(3)}, \widetilde{\sigma}_{d(1)}, \widetilde{\sigma}_{d(6)}, \widehat{C}_{2(1)}, \widehat{C}_{2(2)}, S_{4(3)}, S^3_{4(3)}\} \quad (\supset \mathbf{S}_4) \tag{46}$$

$$\mathbf{C}_{2v\widetilde{\sigma}\widehat{I}} = \{I, C_{2(3)}, \widetilde{\sigma}_{d(1)}, \widetilde{\sigma}_{d(6)}, \widehat{I}, \widehat{C}_{2(3)}, \sigma_{d(1)}, \sigma_{d(6)}\} \quad (\supset \mathbf{C}_{2v}) \tag{47}$$

$$\begin{aligned}\mathbf{C}_{3v\widetilde{\sigma}\widehat{I}} = \{&I, C_{3(1)}, C^2_{3(1)}, \widetilde{\sigma}_{d(1)}, \widetilde{\sigma}_{d(2)}, \widetilde{\sigma}_{d(3)},\\ &\widehat{I}, \widehat{C}_{3(1)}, \widehat{C}^2_{3(1)}, \sigma_{d(1)}, \sigma_{d(2)}, \sigma_{d(3)}\} \quad (\supset \mathbf{C}_{3v})\end{aligned} \tag{48}$$

$$\begin{aligned}\mathbf{D}_{2d\widetilde{\sigma}\widehat{I}} = \{&I, C_{2(1)}, C_{2(2)}, C_{2(3)}, \widetilde{\sigma}_{d(1)}, \widetilde{\sigma}_{d(6)}, \widetilde{S}_{4(3)}, \widetilde{S}^3_{4(3)},\\ &\widehat{I}, \widehat{C}_{2(1)}, \widehat{C}_{2(2)}, \widehat{C}_{2(3)}, \sigma_{d(1)}, \sigma_{d(6)}, S_{4(3)}, S^3_{4(3)}\} \quad (\supset \mathbf{D}_{2d})\end{aligned} \tag{49}$$

$$\mathbf{T}_{d\widetilde{\sigma}\widehat{I}} = \{\mathbf{A}, \mathbf{B}, \mathbf{C}, \mathbf{D}\} \quad (\supset \mathbf{T}_d) \quad \text{(cf. Eq. 5)} \tag{50}$$

The suffix $\widehat{\sigma}$ is used to refer to $\widehat{C}_{2(1)}$ and so on. The symbol $\mathbf{S}_{\widetilde{4}\widehat{\sigma}}$ is based on the subgroup $\mathbf{S}_{\widetilde{4}}$ in place of $\mathbf{C}_{2v}$. The symbol $\mathbf{S}_{\widetilde{4}\widehat{I}}$ is based on the subgroup $\mathbf{S}_{\widetilde{4}}$ in place of $\mathbf{S}_4$. The names of the subgroups are characterized by the symbols with both a hat accent and a tilde accent. These *RS*-stereoisomeric groups are categorized to type IV.

According to the data of Fig. 8, Eq. 28 for the point group $\mathbf{O}_h$ is converted into a non-redundant SSG for $\mathbf{T}_{d\tilde{\sigma}\hat{I}}$:

$$\mathrm{SSG}_{\mathbf{T}_{d\tilde{\sigma}\hat{I}}} = \Big\{ \overset{1}{\mathbf{C}_1}, \overset{2}{\mathbf{C}_2}, \overset{3}{\mathbf{C}_{\tilde{\sigma}}}, \overset{4}{\mathbf{C}_{\hat{\sigma}}}, \overset{5}{\mathbf{C}_s}, \overset{6}{\mathbf{C}_{\hat{I}}}, \overset{7}{\mathbf{C}_3}, \overset{8}{\mathbf{S}_{\tilde{4}}}, \overset{9}{\mathbf{S}_4}, \overset{10}{\mathbf{D}_2}, \overset{11}{\mathbf{C}_{2\tilde{\sigma}}}, \overset{12}{\mathbf{C}_{2\hat{\sigma}}}, \overset{13}{\mathbf{C}_{2v}}, \overset{14}{\mathbf{C}_{s\tilde{\sigma}\hat{\sigma}}}, \overset{15}{\mathbf{C}_{2\hat{I}}}, \overset{16}{\mathbf{C}_{s\tilde{\sigma}\hat{I}}}, \overset{17}{\mathbf{C}_{3\tilde{\sigma}}}, \overset{18}{\mathbf{C}_{3v}}, \overset{19}{\mathbf{C}_{3\hat{I}}}, \overset{20}{\mathbf{D}_{2\tilde{\sigma}}}, \overset{21}{\mathbf{S}_{\tilde{4}\hat{\sigma}}}, \overset{22}{\mathbf{S}_{\tilde{4}\hat{I}}}, \overset{23}{\mathbf{D}_{2d}}, \overset{24}{\mathbf{S}_{4\tilde{\sigma}\hat{\sigma}}}, \overset{25}{\mathbf{D}_{2\hat{I}}}, \overset{26}{\mathbf{C}_{2v\tilde{\sigma}\hat{I}}}, \overset{27}{\mathbf{T}}, \overset{28}{\mathbf{C}_{3v\tilde{\sigma}\hat{I}}}, \overset{29}{\mathbf{D}_{2d\tilde{\sigma}\hat{I}}}, \overset{30}{\mathbf{T}_{\tilde{\sigma}}}, \overset{31}{\mathbf{T}_{\hat{I}}}, \overset{32}{\mathbf{T}_d}, \overset{33}{\mathbf{T}_{d\tilde{\sigma}\hat{I}}} \Big\}, \tag{51}$$

where the subgroups are aligned in the ascending order of their orders. For the convenience of cross reference, sequential numbers from 1 to 33 are attached to the respective subgroups.

4 Subduction of coset representations

4.1 Coset representations of $\mathbf{T}_{d\tilde{\sigma}\hat{I}}$

According to the USCI approach [44], each subgroup $\mathbf{G}_i$ appearing in the $\mathrm{SSG}_{\mathbf{O}_h}$ for the point group $\mathbf{O}_h$ (Eq. 28) corresponds to a coset representation $\mathbf{O}_h(/\mathbf{G}_i)$ of degree $|\mathbf{O}_h|/|\mathbf{G}_i|$. For example, the four diagonals of the cubane skeleton **2** construct an orbit, which is governed by the coset representation $\mathbf{O}_h(/\mathbf{D}_{3d})$ of degree $|\mathbf{O}_h|/|\mathbf{D}_{3d}|$ $(= 48/12 = 4)$. The permutations (products of cycles) of $\mathbf{O}_h(/\mathbf{D}_{3d})$ are collected in Table 1. Note that an overlined permutation (product of cycles) is assigned to a (roto)reflection operation of $\mathbf{O}_h$.

On the same line, each subgroup $\acute{\mathbf{G}}_i$ appearing in the $\mathrm{SSG}_{\mathbf{T}_{d\tilde{\sigma}\hat{I}}}$ for the $\mathbf{T}_{d\tilde{\sigma}\hat{I}}$ (Eq. 51) corresponds to a coset representation $\mathbf{T}_{d\tilde{\sigma}\hat{I}}(/\acute{\mathbf{G}}_i)$ of degree $|\mathbf{T}_{d\tilde{\sigma}\hat{I}}|/|\acute{\mathbf{G}}_i|$. Because $\mathbf{T}_{d\tilde{\sigma}\hat{I}}$ is isomorphic to $\mathbf{O}_h$, the coset representation $\mathbf{T}_{d\tilde{\sigma}\hat{I}}(/\acute{\mathbf{G}}_i)$ consists of an identical set of products of cycles to that of $\mathbf{O}_h(/\mathbf{G}_i)$, if the subgroup $\acute{\mathbf{G}}_i$ $(\subset \mathbf{T}_{d\tilde{\sigma}\hat{I}})$ is selected to be isomorphic to $\mathbf{G}_i$ $(\subset \mathbf{O}_h)$.

For example, the four vertices of the tetrahedral skeleton **1** construct an orbit, which is governed by the coset representation $\mathbf{T}_{d\tilde{\sigma}\hat{I}}(/\mathbf{C}_{3v\tilde{\sigma}\hat{I}})$ of degree $|\mathbf{T}_{d\tilde{\sigma}\hat{I}}|/|\mathbf{C}_{3v\tilde{\sigma}\hat{I}}|$ $(= 48/12 = 4)$. The coset representation $\mathbf{T}_{d\tilde{\sigma}\hat{I}}(/\mathbf{C}_{3v\tilde{\sigma}\hat{I}})$ consists of the same set of products of cycles as $\mathbf{O}_h(/\mathbf{D}_{3d})$ (Table 1), where $\mathbf{C}_{3v\tilde{\sigma}\hat{I}}$ $(\subset \mathbf{T}_{d\tilde{\sigma}\hat{I}})$ is isomorphic to $\mathbf{D}_{3d}$ $(\subset \mathbf{O}_h)$ (cf. Eq. 48).

4.2 Mark table and inverse mark table of $\mathbf{T}_{d\tilde{\sigma}\hat{I}}$

The coset representations $\mathbf{O}_h(/\mathbf{G}_i)$ $(\mathbf{G}_i \in \mathrm{SSG}_{\mathbf{O}_h})$ generate the corresponding mark table $M_{\mathbf{O}_h}$, as reported in Table 1 of [47] and Table 1 of [42]. Because the *RS*-stereoisomeric group $\mathbf{T}_{d\tilde{\sigma}\hat{I}}$ is isomorphic to the point group $\mathbf{O}_h$, the mark table of $\mathbf{T}_{d\tilde{\sigma}\hat{I}}$ represented by the symbol $M_{\mathbf{T}_{d\tilde{\sigma}\hat{I}}}$ can be equalized to the mark table $M_{\mathbf{O}_h}$ as a 33×33 matrix:

$$M_{\mathbf{T}_{d\tilde{\sigma}\hat{I}}} = M_{\mathbf{O}_h} \tag{52}$$

if the $\mathrm{SSG}_{\mathbf{T}_{d\tilde{\sigma}\widehat{I}}}$ (Eq. 51) is selected to be related to the $\mathrm{SSG}_{\mathbf{O}_h}$ (Eq. 28). Hence, the inverse mark table is calculated to be a 33×33 matrix:

$$M^{-1}_{\mathbf{T}_{d\tilde{\sigma}\widehat{I}}} = M^{-1}_{\mathbf{O}_h} = (\overline{m}_{jk})$$

$$= \begin{pmatrix}
1/48 & 0 & 0 & 0 & 0 & 0 & 0 & 0 & 0 & 0 & 0 & 0 & 0 & 0 & 0 & 0 & 0 & 0 & 0 & 0 & 0 & 0 & 0 & 0 & 0 & 0 & 0 & 0 & 0 & 0 & 0 \\
-1/16 & 1/8 & 0 & 0 & 0 & 0 & 0 & 0 & 0 & 0 & 0 & 0 & 0 & 0 & 0 & 0 & 0 & 0 & 0 & 0 & 0 & 0 & 0 & 0 & 0 & 0 & 0 & 0 & 0 & 0 & 0 \\
-1/8 & 0 & 1/4 & 0 & 0 & 0 & 0 & 0 & 0 & 0 & 0 & 0 & 0 & 0 & 0 & 0 & 0 & 0 & 0 & 0 & 0 & 0 & 0 & 0 & 0 & 0 & 0 & 0 & 0 & 0 & 0 \\
-1/16 & 0 & 0 & 1/8 & 0 & 0 & 0 & 0 & 0 & 0 & 0 & 0 & 0 & 0 & 0 & 0 & 0 & 0 & 0 & 0 & 0 & 0 & 0 & 0 & 0 & 0 & 0 & 0 & 0 & 0 & 0 \\
-1/8 & 0 & 0 & 0 & 1/4 & 0 & 0 & 0 & 0 & 0 & 0 & 0 & 0 & 0 & 0 & 0 & 0 & 0 & 0 & 0 & 0 & 0 & 0 & 0 & 0 & 0 & 0 & 0 & 0 & 0 & 0 \\
-1/48 & 0 & 0 & 0 & 0 & 1/24 & 0 & 0 & 0 & 0 & 0 & 0 & 0 & 0 & 0 & 0 & 0 & 0 & 0 & 0 & 0 & 0 & 0 & 0 & 0 & 0 & 0 & 0 & 0 & 0 & 0 \\
-1/12 & 0 & 0 & 0 & 0 & 0 & 1/4 & 0 & 0 & 0 & 0 & 0 & 0 & 0 & 0 & 0 & 0 & 0 & 0 & 0 & 0 & 0 & 0 & 0 & 0 & 0 & 0 & 0 & 0 & 0 & 0 \\
0 & -1/8 & 0 & 0 & 0 & 0 & 0 & 1/4 & 0 & 0 & 0 & 0 & 0 & 0 & 0 & 0 & 0 & 0 & 0 & 0 & 0 & 0 & 0 & 0 & 0 & 0 & 0 & 0 & 0 & 0 & 0 \\
0 & -1/8 & 0 & 0 & 0 & 0 & 0 & 0 & 1/4 & 0 & 0 & 0 & 0 & 0 & 0 & 0 & 0 & 0 & 0 & 0 & 0 & 0 & 0 & 0 & 0 & 0 & 0 & 0 & 0 & 0 & 0 \\
1/24 & -1/8 & 0 & 0 & 0 & 0 & 0 & 0 & 0 & 1/12 & 0 & 0 & 0 & 0 & 0 & 0 & 0 & 0 & 0 & 0 & 0 & 0 & 0 & 0 & 0 & 0 & 0 & 0 & 0 & 0 & 0 \\
1/8 & -1/8 & -1/4 & 0 & 0 & 0 & 0 & 0 & 0 & 0 & 1/4 & 0 & 0 & 0 & 0 & 0 & 0 & 0 & 0 & 0 & 0 & 0 & 0 & 0 & 0 & 0 & 0 & 0 & 0 & 0 & 0 \\
1/8 & -1/8 & 0 & -1/4 & 0 & 0 & 0 & 0 & 0 & 0 & 0 & 1/4 & 0 & 0 & 0 & 0 & 0 & 0 & 0 & 0 & 0 & 0 & 0 & 0 & 0 & 0 & 0 & 0 & 0 & 0 & 0 \\
1/8 & -1/8 & 0 & 0 & -1/4 & 0 & 0 & 0 & 0 & 0 & 0 & 0 & 1/4 & 0 & 0 & 0 & 0 & 0 & 0 & 0 & 0 & 0 & 0 & 0 & 0 & 0 & 0 & 0 & 0 & 0 & 0 \\
1/4 & 0 & -1/4 & -1/4 & -1/4 & 0 & 0 & 0 & 0 & 0 & 0 & 0 & 0 & 1/2 & 0 & 0 & 0 & 0 & 0 & 0 & 0 & 0 & 0 & 0 & 0 & 0 & 0 & 0 & 0 & 0 & 0 \\
1/8 & -1/8 & 0 & -1/8 & 0 & -1/8 & 0 & 0 & 0 & 0 & 0 & 0 & 0 & 0 & 1/4 & 0 & 0 & 0 & 0 & 0 & 0 & 0 & 0 & 0 & 0 & 0 & 0 & 0 & 0 & 0 & 0 \\
1/4 & 0 & -1/4 & 0 & -1/4 & -1/4 & 0 & 0 & 0 & 0 & 0 & 0 & 0 & 0 & 0 & 1/2 & 0 & 0 & 0 & 0 & 0 & 0 & 0 & 0 & 0 & 0 & 0 & 0 & 0 & 0 & 0 \\
1/4 & 0 & -1/2 & 0 & 0 & 0 & -1/4 & 0 & 0 & 0 & 0 & 0 & 0 & 0 & 0 & 0 & 1/2 & 0 & 0 & 0 & 0 & 0 & 0 & 0 & 0 & 0 & 0 & 0 & 0 & 0 & 0 \\
1/4 & 0 & 0 & 0 & -1/2 & 0 & -1/4 & 0 & 0 & 0 & 0 & 0 & 0 & 0 & 0 & 0 & 0 & 1/2 & 0 & 0 & 0 & 0 & 0 & 0 & 0 & 0 & 0 & 0 & 0 & 0 & 0 \\
1/12 & 0 & 0 & 0 & 0 & -1/6 & -1/4 & 0 & 0 & 0 & 0 & 0 & 0 & 0 & 0 & 0 & 0 & 0 & 1/2 & 0 & 0 & 0 & 0 & 0 & 0 & 0 & 0 & 0 & 0 & 0 & 0 \\
0 & 1/4 & 0 & 0 & 0 & 0 & 0 & -1/4 & 0 & -1/4 & -1/4 & 0 & 0 & 0 & 0 & 0 & 0 & 0 & 0 & 1/2 & 0 & 0 & 0 & 0 & 0 & 0 & 0 & 0 & 0 & 0 & 0 \\
0 & 1/4 & 0 & 0 & 0 & 0 & 0 & -1/4 & 0 & 0 & 0 & -1/4 & -1/4 & 0 & 0 & 0 & 0 & 0 & 0 & 0 & 1/2 & 0 & 0 & 0 & 0 & 0 & 0 & 0 & 0 & 0 & 0 \\
0 & 1/4 & 0 & 0 & 0 & 0 & 0 & -1/4 & -1/4 & 0 & 0 & 0 & 0 & -1/4 & 0 & 0 & 0 & 0 & 0 & 0 & 0 & 1/2 & 0 & 0 & 0 & 0 & 0 & 0 & 0 & 0 & 0 \\
0 & 1/4 & 0 & 0 & 0 & 0 & 0 & -1/4 & -1/4 & 0 & 0 & -1/4 & 0 & 0 & 0 & 0 & 0 & 0 & 0 & 0 & 0 & 0 & 1/2 & 0 & 0 & 0 & 0 & 0 & 0 & 0 & 0 \\
0 & 1/4 & 0 & 0 & 0 & 0 & 0 & 0 & -1/4 & 0 & -1/4 & -1/4 & 0 & 0 & 0 & 0 & 0 & 0 & 0 & 0 & 0 & 0 & 0 & 1/2 & 0 & 0 & 0 & 0 & 0 & 0 & 0 \\
-1/6 & 1/4 & 0 & 1/4 & 0 & 1/12 & 0 & 0 & 0 & -1/12 & 0 & -1/4 & 0 & 0 & -1/4 & 0 & 0 & 0 & 0 & 0 & 0 & 0 & 0 & 0 & 1/6 & 0 & 0 & 0 & 0 & 0 & 0 \\
-1/2 & 1/4 & 1/2 & 1/4 & 1/2 & 1/4 & 0 & 0 & 0 & 0 & -1/4 & 0 & -1/4 & -1/2 & -1/4 & -1/2 & 0 & 0 & 0 & 0 & 0 & 0 & 0 & 0 & 0 & 1/2 & 0 & 0 & 0 & 0 & 0 \\
1/12 & 0 & 0 & 0 & 0 & 0 & -1/4 & 0 & 0 & -1/12 & 0 & 0 & 0 & 0 & 0 & 0 & 0 & 0 & 0 & 0 & 0 & 0 & 0 & 0 & 0 & 0 & 1/4 & 0 & 0 & 0 & 0 \\
-1/2 & 0 & 1/2 & 0 & 1/2 & 1/2 & 1/2 & 0 & 0 & 0 & 0 & 0 & 0 & 0 & -1 & -1/2 & -1/2 & -1/2 & 0 & 0 & 0 & 0 & 0 & 0 & 0 & 0 & 1 & 0 & 0 & 0 & 0 \\
0 & -1 & 0 & 0 & 0 & 0 & 0 & 1/2 & 1/2 & 1/2 & 1/2 & 1/2 & 1/2 & 0 & 1/2 & 0 & 0 & 0 & 0 & -1/2 & -1/2 & -1/2 & -1/2 & -1/2 & -1/2 & -1/2 & 0 & 0 & 1 & 0 & 0 & 0 \\
-1/4 & 0 & 1/2 & 0 & 0 & 0 & 1/4 & 0 & 0 & 1/4 & 0 & 0 & 0 & 0 & 0 & -1/2 & 0 & 0 & -1/2 & 0 & 0 & 0 & 0 & 0 & 0 & -1/4 & 0 & 0 & 1/2 & 0 & 0 \\
-1/12 & 0 & 0 & 0 & 0 & 1/6 & 1/4 & 0 & 0 & 1/12 & 0 & 0 & 0 & 0 & 0 & 0 & 0 & -1/2 & 0 & 0 & 0 & 0 & 0 & -1/6 & 0 & -1/4 & 0 & 0 & 0 & 1/2 & 0 \\
-1/4 & 0 & 0 & 0 & 1/2 & 0 & 1/4 & 0 & 0 & 1/4 & 0 & 0 & 0 & 0 & 0 & 0 & -1/2 & 0 & 0 & 0 & 0 & -1/2 & 0 & 0 & 0 & -1/4 & 0 & 0 & 0 & 1/2 & 0 \\
1/2 & 0 & -1/2 & 0 & -1/2 & -1/2 & -1/2 & 0 & 0 & -1/2 & 0 & 0 & 0 & 0 & 1 & 1/2 & 1/2 & 1/2 & 1/2 & 0 & 0 & 1/2 & 0 & 1/2 & 0 & 1/2 & -1 & -1 & -1/2 & -1/2 & -1/2 & 1
\end{pmatrix} \tag{53}$$

which has been previously reported (Table 2 of [47] and Table 2 of [42]).

By obeying the procedure of the USCI approach [44], the four vertices of the tetrahedral skeleton **1** are examined under the respective subgroups of $\mathbf{T}_{d\tilde{\sigma}\widehat{I}}$ to give a fixed-point vector:

$$\begin{aligned} \mathrm{FPV}_1 = (&4, 0, 2, 0, 2, 4, 1, 0, 0, 0, 0, 0, 0, 0, 0, 2, 1, 1, 1, 0, \\ &0, 0, 0, 0, 0, 0, 0, 1, 0, 0, 0, 0, 0) \end{aligned} \tag{54}$$

which is equal to the mark appearing in the $\mathbf{T}_{d\tilde{\sigma}\widehat{I}}(/\mathbf{C}_{3v\tilde{\sigma}\widehat{I}})$-row of the mark table of $\mathbf{T}_{d\tilde{\sigma}\widehat{I}}$. This is equal to the mark appearing in the $\mathbf{O}_h(/\mathbf{D}_{3d})$-row of the mark table of $\mathbf{O}_h$ (Table 1 of [47] and Table 1 of [42]).

To testify that the orbit for the four vertices of the tetrahedral skeleton **1** is governed by $\mathbf{T}_{d\tilde{\sigma}\widehat{I}}(/\mathbf{C}_{3v\tilde{\sigma}\widehat{I}})$-row, the fixed-point vector (Eq. 54) is multiplied by the inverse mark table $M^{-1}_{\mathbf{T}_{d\tilde{\sigma}\widehat{I}}}$ $(= M^{-1}_{\mathbf{O}_h})$ shown in Eq. 4.2, so as to give a vector:

$$\begin{aligned} \mathrm{FPV}_1 \times M^{-1}_{\mathbf{T}_{d\tilde{\sigma}\widehat{I}}} = (&0, 0, 0, 0, 0, 0, 0, 0, 0, 0, 0, 0, 0, 0, 0, 0, 0, 0, 0, 0, 0, \\ &0, 0, 0, 0, 0, 0, 0, 0, 1, 0, 0, 0, 0, 0) \,. \end{aligned} \tag{55}$$

This vector shows the multiplicities of coset representations, so that the value 1 at the 28th position indicates the presence of one coset representation $\mathbf{T}_{d\tilde{\sigma}\widehat{I}}(/\mathbf{C}_{3v\tilde{\sigma}\widehat{I}})$, which corresponds to $\mathbf{O}_h(/\mathbf{D}_{3d})$.

4.3 Subduction and unit subduced cycle indices

4.3.1 Subduction to subgroups of $\mathbf{T}_d$ *related to types III and V*

According to the USCI approach [44], each coset representation $\mathbf{O}_h(/\mathbf{G}_i)$ is subduced into a subgroup $\mathbf{G}_j$. For example, the coset representation $\mathbf{O}_h(/\mathbf{D}_{3d})$ is subduced into its subgroup $\mathbf{G}_j$ ($\in \mathrm{SSG}_{\mathbf{O}_h}$), as collected in the subduction-column of Table 2. The subduction $\mathbf{O}_h(/\mathbf{D}_{3d}) \downarrow \mathbf{G}_j$ is represented by the sum of coset representations of the subgroup $\mathbf{G}_j$, e.g.,

$$\mathbf{O}_h(/\mathbf{D}_{3d}) \downarrow \mathbf{C}'_s = \mathbf{C}'_s(/\mathbf{C}_1) + 2\mathbf{C}'_s(/\mathbf{C}'_s) \tag{56}$$

which appears in the 5th row of Table 2.

According to the formulation of the USCI approach [44], the mark table and its inverse are further used for the subduction of coset representations: $\mathbf{O}_h(/\mathbf{G}_i) \downarrow \mathbf{G}_j$ (for $\mathbf{G}_i, \mathbf{G}_j \in \mathrm{SSG}_{\mathbf{O}_h}$). For example, the subduction of $\mathbf{O}_h(/\mathbf{D}_{3d})$ into $\mathbf{C}'_s$ is conducted by selecting the values for $\mathrm{SSG}_{\mathbf{C}'_s} = \{\mathbf{C}_1, \mathbf{C}'_s\}$ from the $\mathbf{O}_h(/\mathbf{D}_{3d})$-row of the mark table (i.e., Eq. 54). Thereby, we obtain the corresponding mark:

$$M_{\mathbf{O}_h(/\mathbf{D}_{3d})\downarrow\mathbf{C}'_s} = (4, 2), \tag{57}$$

which can be regarded as an FPV for the subgroup $\mathbf{C}'_s$. Because the mark table of $\mathbf{C}'_s$ and its inverse are obtained as follows:

$$M_{\mathbf{C}'_s} = \begin{matrix} \\ \mathbf{C}'_s(/\mathbf{C}_1) \\ \mathbf{C}'_s(/\mathbf{C}'_s) \end{matrix} \begin{matrix} \mathbf{C}_1 & \mathbf{C}'_s \\ \end{matrix} \begin{pmatrix} 2 & 0 \\ 1 & 1 \end{pmatrix}, \quad M^{-1}_{\mathbf{C}'_s} = \begin{pmatrix} \frac{1}{2} & 0 \\ -\frac{1}{2} & 1 \end{pmatrix}, \tag{58}$$

the following multiplication:

$$M_{\mathbf{O}_h(/\mathbf{D}_{3d})\downarrow\mathbf{C}'_s} \times M^{-1}_{\mathbf{C}'_s} = (1, 2) \tag{59}$$

gives the multiplicities of $\mathbf{C}'_s(/\mathbf{C}_1)$ and $\mathbf{C}'_s(/\mathbf{C}'_s)$, as shown in the 5th row of Table 2. This result confirms the subduction represented by Eq. 56. This procedure is repeated to cover all the subgroups contained in $\mathrm{SSG}_{\mathbf{O}_h}$. Thereby, we obtain the subduction column of Table 2.

Because each coset representation generated by the subduction is characterized by a sphericity index (SI), the whole result of the subduction is characterized by a product of SIs, which is called a unit subduced cycle index with chirality fittingness (USCI-CF) according to Def. 9.3 of [44]. For example, Eq. 56 (or Eq. 59) means that the subduction $\mathbf{O}_h(/\mathbf{D}_{3d}) \downarrow \mathbf{C}'_s$ is characterized by a USCI-CF, $a_1^2 c_2$. Similarly, the data collected in the subduction column of Table 2 provide USCI-CFs collected in the USCI-CF column of the same table. When sphericities are not taken into consideration, USCIs (without chirality fittingness) are obtained by putting $s_d = a_d = b_d = c_d$ according to Def. 9.2 of [44], as collected in the USCI column of Table 2. By obeying the procedure exemplified by Table 2, we are able to obtain the full list of the USCI-CFs of $\mathbf{O}_h$, which is shown in Tables 4 and 5 of [42].

Table 2 Subduction of $\mathbf{O}_h(/\mathbf{D}_{3d})$

	Subgroup	Subduction	USCI-CF	USCI	GEM (cf. Eq. 48 of [42])		
	$(\downarrow \mathbf{G}_j)$	$(\mathbf{O}_h/\mathbf{D}_{3d} \downarrow \mathbf{G}_j)$			total $\left(\hat{N}_j\right)$	chiral $\left(\hat{N}_j^{(e)}\right)$	achiral $\left(\hat{N}_j^{(a)}\right)$
1	$\mathbf{C}_1$	$4\mathbf{C}_1\,(/\mathbf{C}_1)$	b_1^4	s_1^4	1/48	1/48	0
2	$\mathbf{C}_2$	$2\mathbf{C}_2\,(/\mathbf{C}_1)$	b_2^2	s_2^2	1/16	1/16	0
3	$\mathbf{C}_2'$	$\mathbf{C}_2'\,(/\mathbf{C}_1) + 2\mathbf{C}_2'\,(/\mathbf{C}_2')$	$b_1^2 b_2$	$s_1^2 s_2$	1/8	1/8	0
4	$\mathbf{C}_s$	$2\mathbf{C}_s\,(/\mathbf{C}_1)$	c_2^2	s_2^2	1/16	−1/16	1/8
5	$\mathbf{C}_s'$	$\mathbf{C}_s'\,(/\mathbf{C}_1) + 2\mathbf{C}_s'\,(/\mathbf{C}_s')$	$a_1^2 c_2$	$s_1^2 s_2$	1/8	−1/8	1/4
6	$\mathbf{C}_i$	$4\mathbf{C}_i\,(/\mathbf{C}_i)$	a_1^4	a_1^4	1/48	−1/48	1/24
7	$\mathbf{C}_3$	$\mathbf{C}_3\,(/\mathbf{C}_1) + \mathbf{C}_3\,(/\mathbf{C}_3)$	$b_1 b_3$	$s_1 s_3$	1/6	1/6	0
8	$\mathbf{C}_4$	$\mathbf{C}_4\,(/\mathbf{C}_1)$	b_4	s_4	1/8	1/8	0
9	$\mathbf{S}_4$	$\mathbf{S}_4\,(/\mathbf{C}_1)$	c_4	s_4	1/8	−1/8	1/4
10	$\mathbf{D}_2$	$\mathbf{D}_2\,(/\mathbf{C}_1)$	b_4	s_4	0	0	0
11	$\mathbf{D}_2'$	$\mathbf{D}_2'\,(/\mathbf{C}_2') + \mathbf{D}_2'\,(/\mathbf{C}_2'')$	b_2^2	s_2^2	0	0	0
12	$\mathbf{C}_{2v}$	$\mathbf{C}_{2v}\,(/\mathbf{C}_1)$	c_4	s_4	0	0	0
13	$\mathbf{C}_{2v}'$	$\mathbf{C}_{2v}'\,(/\mathbf{C}_s) + \mathbf{C}_{2v}'\,(/\mathbf{C}_s')$	a_2^2	s_2^2	0	0	0
14	$\mathbf{C}_{2v}''$	$\mathbf{C}_{2v}''\,(/\mathbf{C}_2') + \mathbf{C}_{2v}''\,(/\mathbf{C}_s')$	$a_2 c_2$	s_2^2	0	0	0
15	$\mathbf{C}_{2h}$	$2\mathbf{C}_{2h}\,(/\mathbf{C}_i)$	a_2^2	s_2^2	0	0	0
16	$\mathbf{C}_{2h}'$	$\mathbf{C}_{2h}'\,(/\mathbf{C}_i) + 2\mathbf{C}_{2h}'\,(/\mathbf{C}_{2h}')$	$a_1^2 a_2$	$s_1^2 s_2$	0	0	0
17	$\mathbf{D}_3$	$\mathbf{D}_3\,(/\mathbf{C}_2) + \mathbf{D}_3\,(/\mathbf{D}_3)$	$b_1 b_3$	$s_1 s_3$	0	0	0
18	$\mathbf{C}_{3v}$	$\mathbf{C}_{3v}\,(/\mathbf{C}_s) + \mathbf{C}_{3v}\,(/\mathbf{C}_{3v})$	$a_1 a_3$	$s_1 s_3$	0	0	0
19	$\mathbf{C}_{3i}$	$\mathbf{C}_{3i}\,(/\mathbf{C}_i) + \mathbf{C}_{3i}\,(/\mathbf{C}_{3i})$	$a_1 a_3$	$s_1 s_3$	1/6	−1/6	1/3
20	$\mathbf{D}_4$	$\mathbf{D}_4\,(/\mathbf{C}_2'')$	b_4	s_4	0	0	0
21	$\mathbf{C}_{4v}$	$\mathbf{C}_{4v}\,(/\mathbf{C}_s')$	a_4	s_4	0	0	0
22	$\mathbf{C}_{4h}$	$\mathbf{C}_{4h}\,(/\mathbf{C}_i)$	a_4	s_4	0	0	0
23	$\mathbf{D}_{2d}$	$\mathbf{D}_{2d}\,(/\mathbf{C}_s)$	a_4	s_4	0	0	0
24	$\mathbf{D}_{2d}'$	$\mathbf{D}_{2d}'\,(/\mathbf{C}_2')$	c_4	s_4	0	0	0
25	$\mathbf{D}_{2h}$	$\mathbf{D}_{2h}\,(/\mathbf{C}_i)$	a_4	s_4	0	0	0
26	$\mathbf{D}_{2h}'$	$\mathbf{D}_{2h}'\,(/\mathbf{C}_{2h}') + \mathbf{D}_{2h}'\,(/\mathbf{C}_{2h}'')$	a_2^2	s_2^2	0	0	0
27	$\mathbf{T}$	$\mathbf{T}\,(/\mathbf{C}_3)$	b_4	s_4	0	0	0
28	$\mathbf{D}_{3d}$	$\mathbf{D}_{3d}\,(/\mathbf{C}_{2h}') + \mathbf{D}_{3d}\,(/\mathbf{D}_{3d})$	$a_1 a_3$	$s_1 s_3$	0	0	0
29	$\mathbf{D}_{4h}$	$\mathbf{D}_{4h}\,(/\mathbf{C}_{2h}')$	a_4	s_4	0	0	0
30	$\mathbf{O}$	$\mathbf{O}\,(/\mathbf{D}_3)$	b_4	s_4	0	0	0
31	$\mathbf{T}_h$	$\mathbf{T}_h\,(/\mathbf{C}_{3i})$	a_4	s_4	0	0	0
32	$\mathbf{T}_d$	$\mathbf{T}_d\,(/\mathbf{C}_{3v})$	a_4	s_4	0	0	0
33	$\mathbf{O}_h$	$\mathbf{O}_h\,(/\mathbf{D}_{3d})$	a_4	s_4	0	0	0

Because the subgroup $\mathbf{C}_s'$ of $\mathbf{O}_h$ is identical with the subgroup $\mathbf{C}_s$ of $\mathbf{T}_{d\tilde{\sigma}\hat{I}}$, the subduction shown by Eq. 56 is written as follows:

$$\mathbf{T}_{d\tilde{\sigma}\hat{I}}(/\mathbf{C}_{3v\tilde{\sigma}\hat{I}}) \downarrow \mathbf{C}_s = \mathbf{C}_s(/\mathbf{C}_1) + 2\mathbf{C}_s(/\mathbf{C}_s) \tag{60}$$

which appears in the 5th row of Table 3. Hence the subduction $\mathbf{T}_{d\tilde{\sigma}\hat{I}}(/\mathbf{C}_{3v\tilde{\sigma}\hat{I}}) \downarrow \mathbf{C}_s$ is characterized by a USCI-CF, $a_1^2 c_2$.

The subductions to the subgroups collected in the $\mathbf{T}_d$(V)-row of Fig. 8 (i.e., $\mathbf{C}_s$, $\mathbf{S}_4$, $\mathbf{C}_{2v}$, $\mathbf{C}_{3v}$, $\mathbf{D}_{2d}$, and $\mathbf{T}_d$) and those collected in the $\mathbf{T}$(III)-row (i.e., $\mathbf{C}_1$, $\mathbf{C}_2$, $\mathbf{C}_3$, $\mathbf{D}_2$, and $\mathbf{T}$) can be discussed in a parallel way, so that the corresponding subduction results and USCI-CFs collected in Table 3 are equivalent to the counterparts collected in Table 2.

4.3.2 Subduction to subgroups of $\mathbf{T}_{\tilde{\sigma}}$ related to type II

Let examine subduction to the subgroups of $\mathbf{T}_{\tilde{\sigma}}$ ($\subset \mathbf{T}_{d\tilde{\sigma}\hat{I}}$), which is isomorphic to $\mathbf{O}$ ($\subset \mathbf{O}_h$). For example, the subduction of $\mathbf{T}_{d\tilde{\sigma}\hat{I}}(/\mathbf{C}_{3v\tilde{\sigma}\hat{I}})$ into $\mathbf{C}_{3\tilde{\sigma}}$ is conducted by selecting the values for

$$\mathrm{SSG}_{\mathbf{C}_{3\tilde{\sigma}}} = \{\mathbf{C}_1, \mathbf{C}_{\tilde{\sigma}}, \mathbf{C}_3, \mathbf{C}_{3\tilde{\sigma}}\} \tag{61}$$

from Eq. 54, which appears in the $\mathbf{T}_{d\tilde{\sigma}\hat{I}}(/\mathbf{C}_{3v\tilde{\sigma}\hat{I}})$-row of the mark table. The first, third, 7th, and 17th values are selected from Eq. 54 to give the corresponding mark:

$$M_{\mathbf{T}_{d\tilde{\sigma}\hat{I}}(/\mathbf{C}_{3v\tilde{\sigma}\hat{I}})\downarrow\mathbf{C}_{3\tilde{\sigma}}} = (4, 2, 1, 2), \tag{62}$$

which can be regarded as an FPV for the subgroup $\mathbf{C}_{3\tilde{\sigma}}$. The mark table of $\mathbf{C}_{3\tilde{\sigma}}$ and its inverse are obtained as follows:

$$M_{\mathbf{C}_{3\tilde{\sigma}}} = \begin{array}{c} \\ \mathbf{C}_{3\tilde{\sigma}}(/\mathbf{C}_1) \\ \mathbf{C}_{3\tilde{\sigma}}(/\mathbf{C}_{\tilde{\sigma}}) \\ \mathbf{C}_{3\tilde{\sigma}}(/\mathbf{C}_3) \\ \mathbf{C}_{3\tilde{\sigma}}(/\mathbf{C}_{3\tilde{\sigma}}) \end{array} \begin{array}{c} \begin{array}{cccc} \mathbf{C}_1 & \mathbf{C}_{\tilde{\sigma}} & \mathbf{C}_3 & \mathbf{C}_{3\tilde{\sigma}} \end{array} \\ \begin{pmatrix} 6 & 0 & 0 & 0 \\ 3 & 1 & 0 & 0 \\ 2 & 0 & 2 & 0 \\ 1 & 1 & 1 & 1 \end{pmatrix} \end{array}, \quad M^{-1}_{\mathbf{C}_{3\tilde{\sigma}}} = \begin{pmatrix} \frac{1}{6} & 0 & 0 & 0 \\ -\frac{1}{2} & 1 & 0 & 0 \\ -\frac{1}{6} & 0 & \frac{1}{2} & 0 \\ \frac{1}{2} & -1 & -\frac{1}{2} & 1 \end{pmatrix}, \tag{63}$$

because $\mathbf{C}_{3\tilde{\sigma}}$ is isomorphic to the point group $\mathbf{D}_3$ (cf. Tables A.12 and B.12 of [44]). Hence, the following multiplication:

$$M_{\mathbf{T}_{d\tilde{\sigma}\hat{I}}(/\mathbf{C}_{3v\tilde{\sigma}\hat{I}})\downarrow\mathbf{C}_{3\tilde{\sigma}}} \times M^{-1}_{\mathbf{C}_{3\tilde{\sigma}}} = (0, 1, 0, 1) \tag{64}$$

gives the subduction:

$$\mathbf{T}_{d\tilde{\sigma}\hat{I}}(/\mathbf{C}_{3v\tilde{\sigma}\hat{I}}) \downarrow \mathbf{C}_{3\tilde{\sigma}} = \mathbf{C}_{3\tilde{\sigma}}(/\mathbf{C}_{\tilde{\sigma}}) + \mathbf{C}_{3\tilde{\sigma}}(/\mathbf{C}_{3\tilde{\sigma}}), \tag{65}$$

which is shown at the 17th row of Table 3. Note that the degrees of the respective coset representations are calculated to be $|\mathbf{C}_{3\tilde{\sigma}}|/|\mathbf{C}_{\tilde{\sigma}}| = 6/2 = 3$ and $|\mathbf{C}_{3\tilde{\sigma}}|/|\mathbf{C}_{3\tilde{\sigma}}| = 6/6 = 1$. Thereby, this subduction gives the USCI-CF $b_1 b_3$ by considering the sphericities of the respective coset representations. This behavior corresponds to the subduction $\mathbf{O}_h(/\mathbf{D}_{3d}) \downarrow \mathbf{D}_3$ shown in the 17th row of Table 2.

Table 3 Subduction of $\mathbf{T}_{d\tilde{\sigma}\hat{I}}(/\mathbf{C}_{3v\tilde{\sigma}\hat{I}})$

	Subgroup	Subduction	USCI-CF	USCI	TEM					
	$(\downarrow \mathbf{G}_j)$	$(\mathbf{T}_{d\tilde{\sigma}\hat{I}}(/\mathbf{C}_{3v\tilde{\sigma}\hat{I}}) \downarrow \mathbf{G}_j)$			$\left(\hat{N}_j\right)$	$\left(\hat{N}_j^I\right)$	$\left(\hat{N}_j^{II}\right)$	$\left(\hat{N}_j^{III}\right)$	$\left(\hat{N}_j^{IV}\right)$	$\left(\hat{N}_j^{V}\right)$
1	$\mathbf{C}_1$	$4\mathbf{C}_1\,(/\mathbf{C}_1)$	b_1^4	s_1^4	1/48	0	0	1/48	0	0
2	$\mathbf{C}_2$	$2\mathbf{C}_2\,(/\mathbf{C}_1)$	b_2^2	s_2^2	1/16	0	0	1/16	0	0
3	$\mathbf{C}_{\tilde{\sigma}}$	$\mathbf{C}_{\tilde{\sigma}}\,(/\mathbf{C}_1) + 2\mathbf{C}_{\tilde{\sigma}}\,(/\mathbf{C}_{\tilde{\sigma}})$	$b_1^2 b_2$	$s_1^2 s_2$	1/8	0	1/4	−1/8	0	0
4	$\mathbf{C}_{\hat{\sigma}}$	$2\mathbf{C}_{\hat{\sigma}}\,(/\mathbf{C}_1)$	c_2^2	s_2^2	1/16	1/8	0	−1/16	0	0
5	$\mathbf{C}_s$	$\mathbf{C}_s\,(/\mathbf{C}_1) + 2\mathbf{C}_s\,(/\mathbf{C}_s)$	$a_1^2 c_2$	$s_1^2 s_2$	1/8	0	0	−1/8	0	1/4
6	$\mathbf{C}_{\hat{I}}$	$4\mathbf{C}_{\hat{I}}\left(/\mathbf{C}_{\hat{I}}\right)$	a_1^4	a_1^4	1/48	1/24	0	−1/48	0	0
7	$\mathbf{C}_3$	$\mathbf{C}_3\,(/\mathbf{C}_1) + \mathbf{C}_3\,(/\mathbf{C}_3)$	$b_1 b_3$	$s_1 s_3$	1/6	0	0	1/6	0	0
8	$\mathbf{S}_{\tilde{4}}$	$\mathbf{S}_{\tilde{4}}\,(/\mathbf{C}_1)$	b_4	s_4	1/8	0	1/4	−1/8	0	0
9	$\mathbf{S}_4$	$\mathbf{S}_4\,(/\mathbf{C}_1)$	c_4	s_4	1/8	0	0	−1/8	0	1/4
10	$\mathbf{D}_2$	$\mathbf{D}_2\,(/\mathbf{C}_1)$	b_4	s_4	0	0	0	0	0	0
11	$\mathbf{C}_{2\tilde{\sigma}}$	$\mathbf{C}_{2\tilde{\sigma}}\left(/\mathbf{C}_{\tilde{\sigma}}\right) + \mathbf{C}_{2\tilde{\sigma}}\left(/\mathbf{C}'_{\tilde{\sigma}}\right)$	b_2^2	s_2^2	0	0	0	0	0	0
12	$\mathbf{C}_{2\hat{\sigma}}$	$\mathbf{C}_{2\hat{\sigma}}\,(/\mathbf{C}_1)$	c_4	s_4	0	0	0	0	0	0
13	$\mathbf{C}_{2v}$	$\mathbf{C}_{2v}\,(/\mathbf{C}_s) + \mathbf{C}_{2v}\,(/\mathbf{C}'_s)$	a_2^2	s_2^2	0	0	0	0	0	0
14	$\mathbf{C}_{s\tilde{\sigma}\hat{\sigma}}$	$\mathbf{C}_{s\tilde{\sigma}\hat{\sigma}}\,(/\mathbf{C}_{\tilde{\sigma}}) + \mathbf{C}_{s\tilde{\sigma}\hat{\sigma}}\,(/\mathbf{C}_s)$	$a_2 c_2$	s_2^2	0	−1/4	−1/4	1/4	1/2	−1/4
15	$\mathbf{C}_{2\hat{I}}$	$2\mathbf{C}_{2\hat{I}}\left(/\mathbf{C}_{\hat{I}}\right)$	a_2^2	s_2^2	0	0	0	0	0	0
16	$\mathbf{C}_{s\tilde{\sigma}\hat{I}}$	$\mathbf{C}_{s\tilde{\sigma}\hat{I}}\left(/\mathbf{C}_{\hat{I}}\right) + 2\mathbf{C}_{s\tilde{\sigma}\hat{I}}\left(/\mathbf{C}_{s\tilde{\sigma}\hat{I}}\right)$	$a_1^2 a_2$	$s_1^2 s_2$	0	−1/4	−1/4	1/4	1/2	−1/4
17	$\mathbf{C}_{3\tilde{\sigma}}$	$\mathbf{C}_{3\tilde{\sigma}}\left(/\mathbf{C}_{\tilde{\sigma}}\right) + \mathbf{C}_{3\tilde{\sigma}}\left(/\mathbf{C}_{3\tilde{\sigma}}\right)$	$b_1 b_3$	$s_1 s_3$	0	0	0	0	0	0
18	$\mathbf{C}_{3v}$	$\mathbf{C}_{3v}\,(/\mathbf{C}_s) + \mathbf{C}_{3v}\,(/\mathbf{C}_{3v})$	$a_1 a_3$	$s_1 s_3$	0	0	0	0	0	0
19	$\mathbf{C}_3^{\hat{I}}$	$\mathbf{C}_{3\hat{I}}\left(/\mathbf{C}_{\hat{I}}\right) + \mathbf{C}_{3\hat{I}}\left(/\mathbf{C}_{3\hat{I}}\right)$	$a_1 a_3$	$s_1 s_3$	1/6	1/3	0	−1/6	0	0
20	$\mathbf{D}_{2\tilde{\sigma}}$	$\mathbf{D}_{2\tilde{\sigma}}\left(/\mathbf{C}_{\tilde{\sigma}}\right)$	b_4	s_4	0	0	0	0	0	0
21	$\mathbf{S}_{\tilde{4}\hat{\sigma}}$	$\mathbf{S}_{\tilde{4}\hat{\sigma}}\,(/\mathbf{C}_s)$	a_4	s_4	0	−1/4	−1/4	1/4	1/2	−1/4

Table 2 continued

	Subgroup	Subduction	USCI-CF	USCI	TEM					
	$(\downarrow \mathbf{G}_j)$	$(\mathbf{T}_{d\tilde{\sigma}\hat{I}}(/\mathbf{C}_{3v\tilde{\sigma}\hat{I}}) \downarrow \mathbf{G}_j)$			$\left(\hat{N}_j\right)$	$\left(\hat{N}_j^I\right)$	$\left(\hat{N}_j^{II}\right)$	$\left(\hat{N}_j^{III}\right)$	$\left(\hat{N}_j^{IV}\right)$	$\left(\hat{N}_j^{V}\right)$
22	$\mathbf{S}_{\tilde{4}\hat{I}}$	$\mathbf{S}_{\tilde{4}\hat{I}}\left(/\mathbf{C}_{\hat{I}}\right)$	a_4	s_4	0	−1/4	−1/4	1/4	1/2	−1/4
23	$\mathbf{D}_{2d}$	$\mathbf{D}_{2d}\ (/\mathbf{C}_s)$	a_4	s_4	0	0	0	0	0	0
24	$\mathbf{S}_{4\tilde{\sigma}\hat{\sigma}}$	$\mathbf{S}_{4\tilde{\sigma}\hat{\sigma}}\ (/\mathbf{C}_{\tilde{\sigma}})$	c_4	s_4	0	−1/4	−1/4	1/4	1/2	−1/4
25	$\mathbf{D}_{2\hat{I}}$	$\mathbf{D}_{2\hat{I}}\left(/\mathbf{C}_{\hat{I}}\right)$	a_4	s_4	0	0	0	0	0	0
26	$\mathbf{C}_{2v\tilde{\sigma}\hat{I}}$	$\mathbf{C}_{2v\tilde{\sigma}\hat{I}}\left(/\mathbf{C}_{s\tilde{\sigma}\hat{I}}\right) + \mathbf{C}_{2v\tilde{\sigma}\hat{I}}\left(/\mathbf{C}'_{s\tilde{\sigma}\hat{I}}\right)$	a_2^2	s_2^2	0	1/4	1/4	−1/4	−1/2	1/4
27	$\mathbf{T}$	$\mathbf{T}\ (/\mathbf{C}_3)$	b_4	s_4	0	0	0	0	0	0
28	$\mathbf{C}_{3v\tilde{\sigma}\hat{I}}$	$\mathbf{C}_{3v\tilde{\sigma}\hat{I}}\left(/\mathbf{C}_{s\tilde{\sigma}\hat{I}}\right) + \mathbf{C}_{3v\tilde{\sigma}\hat{I}}\left(/\mathbf{C}_{3v\tilde{\sigma}\hat{I}}\right)$	$a_1 a_3$	$s_1 s_3$	0	0	0	0	0	0
29	$\mathbf{D}_{2d\tilde{\sigma}\hat{I}}$	$\mathbf{D}_{2d\tilde{\sigma}\hat{I}}\left(/\mathbf{C}_{s\tilde{\sigma}\hat{I}}\right)$	a_4	s_4	0	1/2	1/2	−1/2	−1	1/2
30	$\mathbf{T}_{\tilde{\sigma}}$	$\mathbf{T}_{\tilde{\sigma}}\ (/\mathbf{C}_{3\tilde{\sigma}})$	b_4	s_4	0	0	0	0	0	0
31	$\mathbf{T}_{\hat{I}}$	$\mathbf{T}_{\hat{I}}\left(/\mathbf{C}_{3\hat{I}}\right)$	a_4	s_4	0	0	0	0	0	0
32	$\mathbf{T}_d$	$\mathbf{T}_d\ (/\mathbf{C}_{3v})$	a_4	s_4	0	0	0	0	0	0
33	$\mathbf{T}_{d\tilde{\sigma}\hat{I}}$	$\mathbf{T}_{d\tilde{\sigma}\hat{I}}\left(/\mathbf{C}_{3v\tilde{\sigma}\hat{I}}\right)$	a_4	s_4	0	0	0	0	0	0

The subductions to the subgroups collected in the $\mathbf{T}_{\tilde{\sigma}}$(II)-row of Fig. 8 (i.e., $\mathbf{C}_{\tilde{\sigma}}$, $\mathbf{S}_{\tilde{4}}$, $\mathbf{C}_{2\tilde{\sigma}}$, $\mathbf{C}_{3\tilde{\sigma}}$, $\mathbf{D}_{2\tilde{\sigma}}$, and $\mathbf{T}_{\tilde{\sigma}}$) can be discussed in a parallel way, so that the corresponding subduction results and USCI-CFs collected in Table 3 are equivalent to the counterparts collected in Table 2.

4.3.3 Subduction to subgroups of $\mathbf{T}_{\hat{I}}$ related to type I

Let examine the subduction to the subgroups of $\mathbf{T}_{\hat{I}}$ ($\subset \mathbf{T}_{d\tilde{\sigma}\hat{I}}$), which is isomorphic to $\mathbf{T}_h$ ($\subset \mathbf{O}_h$). For example, the subduction of $\mathbf{T}_{d\tilde{\sigma}\hat{I}}(/\mathbf{C}_{3v\tilde{\sigma}\hat{I}})$ into $\mathbf{C}_{\hat{\sigma}}$ is conducted by selecting the values for

$$\mathrm{SSG}_{\mathbf{C}_{\hat{\sigma}}} = \{\mathbf{C}_1, \mathbf{C}_{\hat{\sigma}}\} \tag{66}$$

from Eq. 54, which appears in the $\mathbf{T}_{d\tilde{\sigma}\hat{I}}(/\mathbf{C}_{3v\tilde{\sigma}\hat{I}})$-row of the mark table. The first and 4th values are selected from Eq. 54 to give the corresponding mark:

$$M_{\mathbf{T}_{d\tilde{\sigma}\hat{I}}(/\mathbf{C}_{3v\tilde{\sigma}\hat{I}})\downarrow\mathbf{C}_{\hat{\sigma}}} = (4, 0), \tag{67}$$

which can be regarded as an FPV for the subgroup $\mathbf{C}_{\hat{\sigma}}$.

The mark table of $\mathbf{C}_{\hat{\sigma}}$ and its inverse are obtained as follows:

$$M_{\mathbf{C}_{\hat{\sigma}}} = \begin{array}{c} \\ \mathbf{C}_{\hat{\sigma}}(/\mathbf{C}_1) \\ \mathbf{C}_{\hat{\sigma}}(/\mathbf{C}'_s) \end{array} \begin{array}{c} \begin{array}{cc} \mathbf{C}_1 & \mathbf{C}_{\hat{\sigma}} \end{array} \\ \begin{pmatrix} 2 & 0 \\ 1 & 1 \end{pmatrix} \end{array}, \quad M^{-1}_{\mathbf{C}_{\hat{\sigma}}} = \begin{pmatrix} \frac{1}{2} & 0 \\ -\frac{1}{2} & 1 \end{pmatrix}, \tag{68}$$

Hence, the following multiplication:

$$M_{\mathbf{T}_{d\tilde{\sigma}\hat{I}}(/\mathbf{C}_{3v\tilde{\sigma}\hat{I}})\downarrow\mathbf{C}_{\hat{\sigma}}} \times M^{-1}_{\mathbf{C}_{\hat{\sigma}}} = (2, 0) \tag{69}$$

gives the multiplicities of $\mathbf{C}_{\hat{\sigma}}(/\mathbf{C}_1)$ and $\mathbf{C}_{\hat{\sigma}}(/\mathbf{C}_{\hat{\sigma}})$. This means that the subduction is represented as follows:

$$\mathbf{T}_{d\tilde{\sigma}\hat{I}}(/\mathbf{C}_{3v\tilde{\sigma}\hat{I}}) \downarrow \mathbf{C}_{\hat{\sigma}} = 2\mathbf{C}_{\hat{\sigma}}(/\mathbf{C}_1), \tag{70}$$

where the degree of the coset representation $\mathbf{C}_{\hat{\sigma}}(/\mathbf{C}_1)$ is calculated to be $|\mathbf{C}_{\hat{\sigma}}|/|\mathbf{C}_1| = 2/1 = 2$. Because the subgroup $\mathbf{C}_{\hat{\sigma}}$ is presumed to be achiral and $\mathbf{C}_1$ is chiral, this subduction gives the USCI-CF c_2^2 by considering the sphericities of the respective coset representations, as listed in the 4th row of Table 3. This behavior corresponds to the subduction $\mathbf{O}_h(/\mathbf{D}_{3d}) \downarrow \mathbf{C}_s$ shown in the 4th row of Table 2.

4.3.4 Subduction to remaining subgroups of $\mathbf{T}_{d\tilde{\sigma}\hat{I}}$ related to type IV

Let examine the subduction to the remaining subgroups of $\mathbf{T}_{d\tilde{\sigma}\hat{I}}$, which are listed in the $\mathbf{T}_{d\tilde{\sigma}\hat{I}}$(IV)-row of Fig. 8. For example, the subduction of $\mathbf{T}_{d\tilde{\sigma}\hat{I}}(/\mathbf{C}_{3v\tilde{\sigma}\hat{I}})$ into the subgroup $\mathbf{C}_{s\tilde{\sigma}\hat{\sigma}}$ (Eq. 42) requires the data of $\mathbf{C}_{s\tilde{\sigma}\hat{\sigma}}$. By considering the isomorphism between $\mathbf{C}_{s\tilde{\sigma}\hat{\sigma}}$ ($\subset \mathbf{T}_{d\tilde{\sigma}\hat{I}}$) and $\mathbf{C}''_{2v}$ ($\subset \mathbf{O}_h$), its SSG is found to be

$$\mathrm{SSG}_{\mathbf{C}_{s\widetilde{\sigma}\widehat{\sigma}}} = \{\mathbf{C}_1, \mathbf{C}_{\widetilde{\sigma}}, \mathbf{C}_{\widehat{\sigma}}, \mathbf{C}_s, \mathbf{C}_{s\widetilde{\sigma}\widehat{\sigma}}\}, \tag{71}$$

the subgroups of which appear in the first, third, 4th, 5th and 14th positions of $\mathrm{SSG}_{\mathbf{T}_{d\widetilde{\sigma}\widehat{I}}}$ (Eq. 51).

According to the USCI approach [44], the mark of this subduction is selected from Eq. 54, which appears in the $\mathbf{T}_{d\widetilde{\sigma}\widehat{I}}(/\mathbf{C}_{3v\widetilde{\sigma}\widehat{I}})$-row of the mark table. The first, third, 4th, 5th and 14th values are selected from Eq. 54 to give the corresponding mark:

$$M_{\mathbf{T}_{d\widetilde{\sigma}\widehat{I}}(/\mathbf{C}_{3v\widetilde{\sigma}\widehat{I}})\downarrow\mathbf{C}_{s\widetilde{\sigma}\widehat{\sigma}}} = (4, 2, 0, 2, 0), \tag{72}$$

which is regarded as an FPV for the subgroup $\mathbf{C}_{s\widetilde{\sigma}\widehat{\sigma}}$.

The mark table of $\mathbf{C}_{s\widetilde{\sigma}\widehat{\sigma}}$ and its inverse are obtained as follows:

$$M_{\mathbf{C}_{s\widetilde{\sigma}\widehat{\sigma}}} = \begin{array}{c} \\ \mathbf{C}_{s\widetilde{\sigma}\widehat{\sigma}}(/\mathbf{C}_1) \\ \mathbf{C}_{s\widetilde{\sigma}\widehat{\sigma}}(/\mathbf{C}_{\widetilde{\sigma}}) \\ \mathbf{C}_{s\widetilde{\sigma}\widehat{\sigma}}(/\mathbf{C}_{\widehat{\sigma}}) \\ \mathbf{C}_{s\widetilde{\sigma}\widehat{\sigma}}(/\mathbf{C}_s) \\ \mathbf{C}_{s\widetilde{\sigma}\widehat{\sigma}}(/\mathbf{C}_{s\widetilde{\sigma}\widehat{\sigma}}) \end{array} \begin{array}{c} \begin{array}{ccccc} \mathbf{C}_1 & \mathbf{C}_{\widetilde{\sigma}} & \mathbf{C}_{\widehat{\sigma}} & \mathbf{C}_s & \mathbf{C}_{s\widetilde{\sigma}\widehat{\sigma}} \end{array} \\ \begin{pmatrix} 4 & 0 & 0 & 0 & 0 \\ 2 & 2 & 0 & 0 & 0 \\ 2 & 0 & 2 & 0 & 0 \\ 2 & 0 & 0 & 2 & 0 \\ 1 & 1 & 1 & 1 & 1 \end{pmatrix} \end{array},$$

$$M^{-1}_{\mathbf{C}_{s\widetilde{\sigma}\widehat{\sigma}}} = \begin{pmatrix} \frac{1}{4} & 0 & 0 & 0 & 0 \\ -\frac{1}{4} & \frac{1}{2} & 0 & 0 & 0 \\ -\frac{1}{4} & 0 & \frac{1}{2} & 0 & 0 \\ -\frac{1}{4} & 0 & 0 & \frac{1}{2} & 0 \\ \frac{1}{2} & -\frac{1}{2} & -\frac{1}{2} & -\frac{1}{2} & 1 \end{pmatrix}, \tag{73}$$

because $\mathbf{C}_{s\widetilde{\sigma}\widehat{\sigma}}$ is isomorphic to the point group $\mathbf{C}_{2v}$ (cf. Tables A.5 and B.5 of [44]). Hence, the following multiplication:

$$M_{\mathbf{T}_{d\widetilde{\sigma}\widehat{I}}(/\mathbf{C}_{3v\widetilde{\sigma}\widehat{I}})\downarrow\mathbf{C}_{s\widetilde{\sigma}\widehat{\sigma}}} \times M^{-1}_{\mathbf{C}_{s\widetilde{\sigma}\widehat{\sigma}}} = (0, 1, 0, 1, 0) \tag{74}$$

gives the subduction:

$$\mathbf{T}_{d\widetilde{\sigma}\widehat{I}}(/\mathbf{C}_{3v\widetilde{\sigma}\widehat{I}}) \downarrow \mathbf{C}_{s\widetilde{\sigma}\widehat{\sigma}} = \mathbf{C}_{s\widetilde{\sigma}\widehat{\sigma}}(/\mathbf{C}_{\widetilde{\sigma}}) + \mathbf{C}_{s\widetilde{\sigma}\widehat{\sigma}}(/\mathbf{C}_s), \tag{75}$$

which is shown at the 14th row of Table 3. This subduction gives the USCI-CF a_2c_2 by considering the sphericities of the respective coset representations. This behavior corresponds to the subduction $\mathbf{O}_h(/\mathbf{D}_{3d}) \downarrow \mathbf{C}''_{2v}$ shown in the 14th row of Table 2.

The subductions to the subgroups collected in the $\mathbf{T}_{d\widetilde{\sigma}\widehat{I}}$(IV)-row of Fig. 8. (i.e., $\mathbf{C}_{s\widetilde{\sigma}\widehat{\sigma}}$, $\mathbf{C}_{s\widetilde{\sigma}\widehat{I}}$, $\mathbf{S}_{\widetilde{4}\widehat{\sigma}}$, $\mathbf{S}_{\widetilde{4}\widehat{I}}$, $\mathbf{S}_{4\widetilde{\sigma}\widehat{\sigma}}$, $\mathbf{C}_{2v\widetilde{\sigma}\widehat{I}}$, $\mathbf{C}_{3v\widetilde{\sigma}\widehat{I}}$, $\mathbf{D}_{2d\widetilde{\sigma}\widehat{I}}$, and $\mathbf{T}_{d\widetilde{\sigma}\widehat{I}}$) can be discussed in a parallel way, so that the corresponding subduction results and USCI-CFs collected in Table 3 are equivalent to the counterparts collected in Table 2.

5 Symmetry-itemized enumeration

5.1 Fixed-point vectors for symmetry-itemized enumeration

A subduced cycle index with chirality fittingness (SCI-CF) defined as a product of USCI-CFs (Def. 19.3 of [44]) is capable of evaluating the number of fixed promolecules as *RS*-stereoisomers. Such an SCI-CF is identical with the corresponding USCI-CF (the USCI-CF-column of Fig. 3) in the present enumeration of *RS*-stereoisomers, because there exists a single orbit.

Suppose that substituents for the four positions of **1** are selected from an inventory of proligands:

$$\mathbf{X} = \{\mathrm{A}, \mathrm{B}, \mathrm{X}, \mathrm{Y};\quad \mathrm{p}, \mathrm{q}, \mathrm{r}, \mathrm{s};\quad \overline{\mathrm{p}}, \overline{\mathrm{q}}, \overline{\mathrm{r}}, \overline{\mathrm{s}}\}, \tag{76}$$

where the letters A, B, X, and Y represent achiral proligands and the pairs of p/$\overline{\mathrm{p}}$, q/$\overline{\mathrm{q}}$, r/$\overline{\mathrm{r}}$, and s/$\overline{\mathrm{s}}$ represent pairs of enantiomeric proligands in isolation. According to Lemma 19.2 of [44], we use the following ligand-inventory functions:

$$a_d = \mathrm{A}^d + \mathrm{B}^d + \mathrm{X}^d + \mathrm{Y}^d \tag{77}$$

$$c_d = \mathrm{A}^d + \mathrm{B}^d + \mathrm{X}^d + \mathrm{Y}^d + 2\mathrm{p}^{d/2}\overline{\mathrm{p}}^{d/2} + 2\mathrm{q}^{d/2}\overline{\mathrm{q}}^{d/2} + 2\mathrm{r}^{d/2}\overline{\mathrm{r}}^{d/2} + 2\mathrm{s}^{d/2}\overline{\mathrm{s}}^{d/2} \tag{78}$$

$$b_d = \mathrm{A}^d + \mathrm{B}^d + \mathrm{X}^d + \mathrm{Y}^d + \mathrm{p}^d + \mathrm{q}^d + \mathrm{r}^d + \mathrm{s}^d + \overline{\mathrm{p}}^d + \overline{\mathrm{q}}^d + \overline{\mathrm{r}}^d + \overline{\mathrm{s}}^d. \tag{79}$$

It should be noted that the power $d/2$ appearing in Eq. 78 is an integer because the subscript d of c_d is always even in the light of the enantiosphericity of the corresponding orbit. These ligand-inventory functions are introduced into an SCI-CF to give a generating function, in which the coefficient of the term $\mathrm{A}^a\mathrm{B}^b\mathrm{X}^x\mathrm{Y}^y\mathrm{p}^p\overline{\mathrm{p}}^{\overline{p}}\mathrm{q}^q\overline{\mathrm{q}}^{\overline{q}}\mathrm{r}^r\overline{\mathrm{q}}^{\overline{r}}\mathrm{s}^s\overline{\mathrm{q}}^{\overline{s}}$ indicates the number of fixed promolecules to be counted. Because A, B, etc. appear symmetrically, the term can be represented by the following partition:

$$[\theta] = [a, b, x, y; p, \overline{p}, q, \overline{q}, r, \overline{r}, s, \overline{s}], \tag{80}$$

where we put $a \geq b \geq x \geq y$, $p \geq \overline{p}$, $q \geq \overline{q}$, $r \geq \overline{r}$, $s \geq \overline{s}$, and $p \geq q \geq r \geq s$ without losing generality.

For example, let us examine the SCI-CF (USCI-CF) for $\mathbf{T}_{d\widetilde{\sigma}\widehat{I}}(/\mathbf{C}_{3v\widetilde{\sigma}\widehat{I}}) \downarrow \mathbf{C}_s$, i.e., $a_1^2c_2$, into which the ligand-inventory functions (Eqs. 77–79) are introduced. The resulting equation is expanded to give the following generating function:

$$\begin{aligned} g_{\mathbf{C}_s} &= (\mathrm{A} + \mathrm{B} + \mathrm{X} + \mathrm{Y})^2(\mathrm{A}^2 + \mathrm{B}^2 + \mathrm{X}^2 + \mathrm{Y}^2 + 2\mathrm{p}\overline{\mathrm{p}} + 2\mathrm{q}\overline{\mathrm{q}} + 2\mathrm{r}\overline{\mathrm{r}} + 2\mathrm{s}\overline{\mathrm{s}}) \\ &= \{\mathrm{A}^4 + \mathrm{B}^4 + \mathrm{X}^4 + \mathrm{Y}^4\} + \{2\mathrm{A}^3\mathrm{B} + 2\mathrm{A}^3\mathrm{X} + 2 * \mathrm{A}^3\mathrm{Y} + \cdots\} \\ &\quad + \{2\mathrm{A}^2\mathrm{B}^2 + 2\mathrm{A}^2\mathrm{X}^2 + \cdots\} + \{2\mathrm{A}^2\mathrm{BX} + 2\mathrm{A}^2\mathrm{BY} + \cdots\} \\ &\quad + \{2\mathrm{A}^2\mathrm{p}\overline{\mathrm{p}} + 2\mathrm{A}^2\mathrm{q}\overline{\mathrm{q}} + \cdots\} + \{4\mathrm{ABp}\overline{\mathrm{p}} + 4\mathrm{ABq}\overline{\mathrm{q}} + \cdots\} \end{aligned} \tag{81}$$

Among these terms, for example, we focus our attention on A^4 (as a representative of the first pair of braces) and $2A^3B$ (as a representative of the second pair of braces). The coefficient 1 of A^4 means that one promolecule with the formula A^4 or the partition:

$$[\theta]_1 = [4, 0, 0, 0; 0, 0, 0, 0, 0, 0, 0, 0] \tag{82}$$

is fixed under the action of $\mathbf{C}_s$. The coefficient 2 of A^3B means that two promolecule with the formula A^3B or the partition:

$$[\theta]_2 = [3, 1, 0, 0; 0, 0, 0, 0, 0, 0, 0, 0] \tag{83}$$

are fixed under the action of $\mathbf{C}_s$. These results are symbolically represented as follows:

$$\rho_{[\theta]_1\mathbf{C}_s} = 1 \tag{84}$$
$$\rho_{[\theta]_2\mathbf{C}_s} = 2 \tag{85}$$

This procedure is repeated to cover all the subgroups contained in $\mathrm{SSG}_{\mathbf{T}_{d\tilde{\sigma}\hat{I}}}$ (Eq. 51). Thereby, we obtain $\rho_{[\theta]_1\acute{\mathbf{G}}_j}$ for $\acute{\mathbf{G}}_j$ ($\in \mathrm{SSG}_{\mathbf{T}_{d\tilde{\sigma}\hat{I}}}$), which are collected so as to give an FPV for symmetry-itemized enumeration for the partition $[\theta]_1$:

$$\begin{aligned}
&\mathrm{FPV}_{[\theta]_1} \\
&= (\rho_{[\theta]_1\mathbf{C}_1}, \ldots, \rho_{[\theta]_1\mathbf{C}_s}, \ldots, \rho_{[\theta]_1\acute{\mathbf{G}}_j}, \ldots, \rho_{[\theta]_1\mathbf{T}_{d\tilde{\sigma}\hat{I}}}) \\
&= (1, 1, 1, 1, 1, 1, 1, 1, 1, 1, 1, 1, 1, 1, 1, 1, 1, 1, 1, 1, 1, 1, 1, 1, 1, 1, 1, \\
&\quad 1, 1, 1, 1, 1).
\end{aligned} \tag{86}$$

Similarly, another FPV for symmetry-itemized enumeration for the partition $[\theta]_2$ is obtained:

$$\begin{aligned}
&\mathrm{FPV}_{[\theta]_2} \\
&= (\rho_{[\theta]_2\mathbf{C}_1}, \ldots, \rho_{[\theta]_2\mathbf{C}_s}, \ldots, \rho_{[\theta]_2\acute{\mathbf{G}}_j}, \ldots, \rho_{[\theta]_2\mathbf{T}_{d\tilde{\sigma}\hat{I}}}) \\
&= (4, 0, 2, 0, 2, 4, 1, 0, 0, 0, 0, 0, 0, 0, 0, 2, 1, 1, 1, 0, 0, 0, 0, 0, 0, 0, 0, 1, 0, \\
&\quad 0, 0, 0, 0).
\end{aligned} \tag{87}$$

Note that the values $\rho_{[\theta]_1\mathbf{C}_s}$ (Eq. 84) and $\rho_{[\theta]_2\mathbf{C}_s}$ (Eq. 85) appear at the 5th positions of the respective FPVs (Eqs. 86 and 87).

According to Theorem 19.4 (coupled with Theorem 15.4) in [44], the FPVs are multiplied by the inverse $M^{-1}_{\mathbf{T}_{d\tilde{\sigma}\hat{I}}}$ (Eq. 4.2) to give the following isomer-counting vectors (ICVs):

$$\begin{aligned}\mathrm{ICV}_{[\theta]_1} &= \mathrm{FPV}_{[\theta]_1} \times M^{-1}_{\mathbf{T}_{d\widetilde{\sigma}\widehat{I}}} \\ &= (0, 0, 0, 0, 0, 0, 0, 0, 0, 0, 0, 0, 0, 0, 0, 0, 0, 0, 0, 0, 0, 0, 0, 0, 0, 0, 0, \\ &\quad 0, 0, 0, 0, 0, 1), \end{aligned} \tag{88}$$

$$\begin{aligned}\mathrm{ICV}_{[\theta]_2} &= \mathrm{FPV}_{[\theta]_2} \times M^{-1}_{\mathbf{T}_{d\widetilde{\sigma}\widehat{I}}} \\ &= (0, 0, 0, 0, 0, 0, 0, 0, 0, 0, 0, 0, 0, 0, 0, 0, 0, 0, 0, 0, 0, 0, 0, 0, 0, 0, 0, 0, 1, 0, \\ &\quad 0, 0, 0, 0). \end{aligned} \tag{89}$$

By referring to $\mathrm{SSG}_{\mathbf{T}_{d\widetilde{\sigma}\widehat{I}}}$ (Eq. 51), Eq. 88 indicates that one promolecule (a quadruplet) as an *RS*-stereoisomer with $[\theta]_1$ (A^4 etc.) exists to belong to $\mathbf{T}_{d\widetilde{\sigma}\widehat{I}}$, while Eq. 89 indicates that one promolecule (a quadruplet) as an *RS*-stereoisomer with $[\theta]_2$ (A^3B etc.) exists to belong to $\mathbf{C}_{3v\widetilde{\sigma}\widehat{I}}$.

5.2 Fixed-point matrices for symmetry-itemized enumeration

For the purpose of systematic enumeration, several FPVs can be collected as row vectors of a matrix, which is called *a fixed-point matrix* (FPM) according to Sections 15.2 and 19.2 of [44]. For example, such an FPM as corresponding to the following partitions:

$$[\theta]_1 = [4, 0, 0, 0; 0, 0, 0, 0, 0, 0, 0, 0] \quad (\text{for } A^4 \text{ etc.}) \tag{90}$$
$$[\theta]_2 = [3, 1, 0, 0; 0, 0, 0, 0, 0, 0, 0, 0] \quad (\text{for } A^3B \text{ etc.}) \tag{91}$$
$$[\theta]_3 = [3, 0, 0, 0; 1, 0, 0, 0, 0, 0, 0, 0] \quad (\text{for } A^3p \text{ etc.}) \tag{92}$$
$$[\theta]_4 = [2, 2, 0, 0; 0, 0, 0, 0, 0, 0, 0, 0] \quad (\text{for } A^2B^2 \text{ etc.}) \tag{93}$$
$$[\theta]_5 = [2, 0, 0, 0; 2, 0, 0, 0, 0, 0, 0, 0] \quad (\text{for } A^2p^2 \text{ etc.}) \tag{94}$$
$$[\theta]_6 = [2, 1, 1, 0; 0, 0, 0, 0, 0, 0, 0, 0] \quad (\text{for } A^2BX \text{ etc.}) \tag{95}$$
$$[\theta]_7 = [2, 1, 0, 0; 1, 0, 0, 0, 0, 0, 0, 0] \quad (\text{for } A^2\,Bp \text{ etc.}) \tag{96}$$
$$[\theta]_8 = [2, 0, 0, 0; 1, 1, 0, 0, 0, 0, 0, 0] \quad (\text{for } A^2p\overline{p} \text{ etc.}) \tag{97}$$
$$[\theta]_9 = [2, 0, 0, 0; 1, 0, 1, 0, 0, 0, 0, 0] \quad (\text{for } A^2pq \text{ etc.}) \tag{98}$$
$$[\theta]_{10} = [1, 1, 1, 1; 0, 0, 0, 0, 0, 0, 0, 0] \quad (\text{for } ABXY) \tag{99}$$
$$[\theta]_{11} = [1, 1, 1, 0; 1, 0, 0, 0, 0, 0, 0, 0] \quad (\text{for } ABXp \text{ etc.}) \tag{100}$$
$$[\theta]_{12} = [1, 1, 0, 0; 2, 0, 0, 0, 0, 0, 0, 0] \quad (\text{for } ABp^2 \text{ etc.}) \tag{101}$$
$$[\theta]_{13} = [1, 1, 0, 0; 1, 1, 0, 0, 0, 0, 0, 0] \quad (\text{for } ABp\overline{p} \text{ etc.}) \tag{102}$$
$$[\theta]_{14} = [1, 1, 0, 0; 1, 0, 1, 0, 0, 0, 0, 0] \quad (\text{for } ABpq \text{ etc.}) \tag{103}$$
$$[\theta]_{15} = [1, 0, 0, 0; 3, 0, 0, 0, 0, 0, 0, 0] \quad (\text{for } Ap^3 \text{ etc.}) \tag{104}$$
$$[\theta]_{16} = [1, 0, 0, 0; 2, 1, 0, 0, 0, 0, 0, 0] \quad (\text{for } Ap^2\overline{p} \text{ etc.}) \tag{105}$$
$$[\theta]_{17} = [1, 0, 0, 0; 2, 0, 1, 0, 0, 0, 0, 0] \quad (\text{for } Ap^2q \text{ etc.}) \tag{106}$$
$$[\theta]_{18} = [1, 0, 0, 0; 1, 1, 1, 0, 0, 0, 0, 0] \quad (\text{for } Ap\overline{p}q \text{ etc.}) \tag{107}$$
$$[\theta]_{19} = [1, 0, 0, 0; 1, 0, 1, 0, 1, 0, 0, 0] \quad (\text{for } Apqr \text{ etc.}) \tag{108}$$

can be constructed from the data of generating functions (e.g., Eq. 81) by applying the procedure described above (cf. Eqs. 86 and 87 for obtaining $\mathrm{FPV}_{[\theta]_1}$ and $\mathrm{FPV}_{[\theta]_2}$). Thereby, we obtain the following FPM:

$$
\mathrm{FPM}_1 = \begin{array}{c} \\ [\theta]_1 \\ [\theta]_2 \\ [\theta]_3 \\ [\theta]_4 \\ [\theta]_5 \\ [\theta]_6 \\ [\theta]_7 \\ [\theta]_8 \\ [\theta]_9 \\ [\theta]_{10} \\ [\theta]_{11} \\ [\theta]_{12} \\ [\theta]_{13} \\ [\theta]_{14} \\ [\theta]_{15} \\ [\theta]_{16} \\ [\theta]_{17} \\ [\theta]_{18} \\ [\theta]_{19} \end{array}
\begin{pmatrix}
1 & 1 & 1 & 1 & 1 & 1 & 1 & 1 & 1 & 1 & 1 & 1 & 1 & 1 & 1 & 1 & 1 & 1 & 1 & 1 & 1 & 1 & 1 & 1 & 1 & 1 & 1 & 1 & 1 & 1 \\
4 & 0 & 2 & 0 & 2 & 4 & 1 & 0 & 0 & 0 & 0 & 0 & 0 & 0 & 0 & 2 & 1 & 1 & 1 & 0 & 0 & 0 & 0 & 0 & 0 & 0 & 0 & 1 & 0 & 0 & 0 & 0 & 0 \\
4 & 0 & 2 & 0 & 0 & 0 & 1 & 0 & 0 & 0 & 0 & 0 & 0 & 0 & 0 & 0 & 1 & 0 & 0 & 0 & 0 & 0 & 0 & 0 & 0 & 0 & 0 & 0 & 0 & 0 & 0 & 0 & 0 \\
6 & 2 & 2 & 2 & 2 & 6 & 0 & 0 & 0 & 0 & 2 & 0 & 2 & 2 & 2 & 2 & 0 & 0 & 0 & 0 & 0 & 0 & 0 & 0 & 0 & 2 & 0 & 0 & 0 & 0 & 0 & 0 & 0 \\
6 & 2 & 2 & 0 & 0 & 0 & 0 & 0 & 0 & 0 & 2 & 0 & 0 & 0 & 0 & 0 & 0 & 0 & 0 & 0 & 0 & 0 & 0 & 0 & 0 & 0 & 0 & 0 & 0 & 0 & 0 & 0 & 0 \\
12 & 0 & 2 & 0 & 2 & 12 & 0 & 0 & 0 & 0 & 0 & 0 & 0 & 0 & 0 & 2 & 0 & 0 & 0 & 0 & 0 & 0 & 0 & 0 & 0 & 0 & 0 & 0 & 0 & 0 & 0 & 0 & 0 \\
12 & 0 & 2 & 0 & 0 & 0 & 0 & 0 & 0 & 0 & 0 & 0 & 0 & 0 & 0 & 0 & 0 & 0 & 0 & 0 & 0 & 0 & 0 & 0 & 0 & 0 & 0 & 0 & 0 & 0 & 0 & 0 & 0 \\
12 & 0 & 2 & 4 & 2 & 0 & 0 & 0 & 0 & 0 & 0 & 0 & 2 & 0 & 0 & 0 & 0 & 0 & 0 & 0 & 0 & 0 & 0 & 0 & 0 & 0 & 0 & 0 & 0 & 0 & 0 & 0 & 0 \\
12 & 0 & 2 & 0 & 0 & 0 & 0 & 0 & 0 & 0 & 0 & 0 & 0 & 0 & 0 & 0 & 0 & 0 & 0 & 0 & 0 & 0 & 0 & 0 & 0 & 0 & 0 & 0 & 0 & 0 & 0 & 0 & 0 \\
24 & 0 & 0 & 0 & 0 & 24 & 0 & 0 & 0 & 0 & 0 & 0 & 0 & 0 & 0 & 0 & 0 & 0 & 0 & 0 & 0 & 0 & 0 & 0 & 0 & 0 & 0 & 0 & 0 & 0 & 0 & 0 & 0 \\
24 & 0 & 0 & 0 & 0 & 0 & 0 & 0 & 0 & 0 & 0 & 0 & 0 & 0 & 0 & 0 & 0 & 0 & 0 & 0 & 0 & 0 & 0 & 0 & 0 & 0 & 0 & 0 & 0 & 0 & 0 & 0 & 0 \\
12 & 0 & 2 & 0 & 0 & 0 & 0 & 0 & 0 & 0 & 0 & 0 & 0 & 0 & 0 & 0 & 0 & 0 & 0 & 0 & 0 & 0 & 0 & 0 & 0 & 0 & 0 & 0 & 0 & 0 & 0 & 0 & 0 \\
24 & 0 & 0 & 0 & 4 & 0 & 0 & 0 & 0 & 0 & 0 & 0 & 0 & 0 & 0 & 0 & 0 & 0 & 0 & 0 & 0 & 0 & 0 & 0 & 0 & 0 & 0 & 0 & 0 & 0 & 0 & 0 & 0 \\
24 & 0 & 0 & 0 & 0 & 0 & 0 & 0 & 0 & 0 & 0 & 0 & 0 & 0 & 0 & 0 & 0 & 0 & 0 & 0 & 0 & 0 & 0 & 0 & 0 & 0 & 0 & 0 & 0 & 0 & 0 & 0 & 0 \\
4 & 0 & 2 & 0 & 0 & 0 & 1 & 0 & 0 & 0 & 0 & 0 & 0 & 0 & 0 & 0 & 1 & 0 & 0 & 0 & 0 & 0 & 0 & 0 & 0 & 0 & 0 & 0 & 0 & 0 & 0 & 0 & 0 \\
12 & 0 & 2 & 0 & 0 & 0 & 0 & 0 & 0 & 0 & 0 & 0 & 0 & 0 & 0 & 0 & 0 & 0 & 0 & 0 & 0 & 0 & 0 & 0 & 0 & 0 & 0 & 0 & 0 & 0 & 0 & 0 & 0 \\
12 & 0 & 2 & 0 & 0 & 0 & 0 & 0 & 0 & 0 & 0 & 0 & 0 & 0 & 0 & 0 & 0 & 0 & 0 & 0 & 0 & 0 & 0 & 0 & 0 & 0 & 0 & 0 & 0 & 0 & 0 & 0 & 0 \\
24 & 0 & 0 & 0 & 0 & 0 & 0 & 0 & 0 & 0 & 0 & 0 & 0 & 0 & 0 & 0 & 0 & 0 & 0 & 0 & 0 & 0 & 0 & 0 & 0 & 0 & 0 & 0 & 0 & 0 & 0 & 0 & 0 \\
24 & 0 & 0 & 0 & 0 & 0 & 0 & 0 & 0 & 0 & 0 & 0 & 0 & 0 & 0 & 0 & 0 & 0 & 0 & 0 & 0 & 0 & 0 & 0 & 0 & 0 & 0 & 0 & 0 & 0 & 0 & 0 & 0
\end{pmatrix}
\tag{109}
$$

where the values collected in each column appear as the coefficients of the terms which correspond to the partitions $[\theta]_i$ ($i = 1$–19), appearing in the generating function of the *RS*-stereoisomeric group of the column. Thus, the coefficients of respective terms in the generating function $g_{\mathbf{C}_s}$ (Eq. 81) appear in the $\mathbf{C}_s$-column (the 5th column) of the FPM_1 (Eq. 109), where non-zero values appear in the $[\theta]_1$-row (for A^4 etc.), the $[\theta]_2$-row (for $\mathrm{A}^3\mathrm{B}$ etc.), the $[\theta]_4$-row (for $\mathrm{A}^2\mathrm{B}^2$ etc.), the $[\theta]_6$-row (for $\mathrm{A}^2\mathrm{BX}$ etc.), the $[\theta]_8$-row (for $\mathrm{A}^2\mathrm{p}\,\overline{\mathrm{p}}$ etc.), and the $[\theta]_{13}$-row (for $\mathrm{ABp}\overline{\mathrm{p}}$ etc.).

Because the FPM (Eq. 109) contains FPVs as its row vectors, it is multiplied by the inverse $M^{-1}_{\mathbf{T}_{d\tilde{\sigma}\hat{I}}}$ (Eq. 4.2), so as to give an isomer-counting matrix (ICM_1):

$$
\begin{aligned}
\mathrm{ICM}_1 &= \mathrm{FPM}_1 \times M^{-1}_{\mathbf{T}_{d\tilde{\sigma}\hat{I}}} \\
&= \begin{array}{c}
[\theta]_1 \\ [\theta]_2 \\ [\theta]_3 \\ [\theta]_4 \\ [\theta]_5 \\ [\theta]_6 \\ [\theta]_7 \\ [\theta]_8 \\ [\theta]_9 \\ [\theta]_{10} \\ [\theta]_{11} \\ [\theta]_{12} \\ [\theta]_{13} \\ [\theta]_{14} \\ [\theta]_{15} \\ [\theta]_{16} \\ [\theta]_{17} \\ [\theta]_{18} \\ [\theta]_{19}
\end{array}
\begin{pmatrix}
0 & 0\,0 & 0\,0\,0\,0\,0\,0\,0\,0\,0 & 0\,0\,0\,0\,0\,0 & 0\,0\,0\,0\,0\,0\,0\,0\,0\,0\,0\,0\,0\,0\,0 & 1 \\
0 & 0\,0 & 0\,0\,0\,0\,0\,0\,0\,0\,0 & 0\,0\,0\,0\,0\,0 & 0\,0\,0\,0\,0\,0\,0\,0\,0\,0\,0\,0\,0\,0\,1 & 0\,0\,0\,0\,0\,0 \\
0 & 0\,0 & 0\,0\,0\,0\,0\,0\,0\,0\,0 & 0\,0\,0\,0\,0\,1/2 & 0\,0\,0\,0\,0\,0\,0\,0\,0\,0\,0\,0\,0\,0\,0 & 0\,0\,0\,0\,0\,0 \\
0 & 0\,0 & 0\,0\,0\,0\,0\,0\,0\,0\,0 & 0\,0\,0\,0\,0\,0 & 0\,0\,0\,0\,0\,0\,0\,0\,1 & 0\,0\,0\,0\,0\,0\,0 \\
0 & 0\,0 & 0\,0\,0\,0\,0\,0\,0\,0\,1/2 & 0\,0\,0\,0\,0\,0 & 0\,0\,0\,0\,0\,0\,0\,0\,0\,0\,0\,0\,0\,0\,0 & 0\,0\,0\,0\,0\,0 \\
0 & 0\,0 & 0\,0\,0\,0\,0\,0\,0\,0\,0 & 0\,0\,0\,0\,1\,0 & 0\,0\,0\,0\,0\,0\,0\,0\,0\,0\,0\,0\,0\,0\,0 & 0\,0\,0\,0\,0\,0 \\
0 & 0\,1/2 & 0\,0\,0\,0\,0\,0\,0\,0\,0 & 0\,0\,0\,0\,0\,0 & 0\,0\,0\,0\,0\,0\,0\,0\,0\,0\,0\,0\,0\,0\,0 & 0\,0\,0\,0\,0\,0 \\
0 & 0\,0 & 0\,0\,0\,0\,0\,0\,0\,0\,0 & 0\,0\,1\,0\,0\,0 & 0\,0\,0\,0\,0\,0\,0\,0\,0\,0\,0\,0\,0\,0\,0 & 0\,0\,0\,0\,0\,0 \\
0 & 0\,1/2 & 0\,0\,0\,0\,0\,0\,0\,0\,0 & 0\,0\,0\,0\,0\,0 & 0\,0\,0\,0\,0\,0\,0\,0\,0\,0\,0\,0\,0\,0\,0 & 0\,0\,0\,0\,0\,0 \\
0 & 0\,0 & 0\,0\,1\,0\,0\,0\,0\,0\,0 & 0\,0\,0\,0\,0\,0 & 0\,0\,0\,0\,0\,0\,0\,0\,0\,0\,0\,0\,0\,0\,0 & 0\,0\,0\,0\,0\,0 \\
1/2 & 0\,0 & 0\,0\,0\,0\,0\,0\,0\,0\,0 & 0\,0\,0\,0\,0\,0 & 0\,0\,0\,0\,0\,0\,0\,0\,0\,0\,0\,0\,0\,0\,0 & 0\,0\,0\,0\,0\,0 \\
0 & 0\,1/2 & 0\,0\,0\,0\,0\,0\,0\,0\,0 & 0\,0\,0\,0\,0\,0 & 0\,0\,0\,0\,0\,0\,0\,0\,0\,0\,0\,0\,0\,0\,0 & 0\,0\,0\,0\,0\,0 \\
0 & 0\,0 & 0\,1\,0\,0\,0\,0\,0\,0\,0 & 0\,0\,0\,0\,0\,0 & 0\,0\,0\,0\,0\,0\,0\,0\,0\,0\,0\,0\,0\,0\,0 & 0\,0\,0\,0\,0\,0 \\
1/2 & 0\,0 & 0\,0\,0\,0\,0\,0\,0\,0\,0 & 0\,0\,0\,0\,0\,0 & 0\,0\,0\,0\,0\,0\,0\,0\,0\,0\,0\,0\,0\,0\,0 & 0\,0\,0\,0\,0\,0 \\
0 & 0\,0 & 0\,0\,0\,0\,0\,0\,0\,0\,0 & 0\,0\,0\,0\,0\,1/2 & 0\,0\,0\,0\,0\,0\,0\,0\,0\,0\,0\,0\,0\,0\,0 & 0\,0\,0\,0\,0\,0 \\
0 & 0\,1/2 & 0\,0\,0\,0\,0\,0\,0\,0\,0 & 0\,0\,0\,0\,0\,0 & 0\,0\,0\,0\,0\,0\,0\,0\,0\,0\,0\,0\,0\,0\,0 & 0\,0\,0\,0\,0\,0 \\
0 & 0\,1/2 & 0\,0\,0\,0\,0\,0\,0\,0\,0 & 0\,0\,0\,0\,0\,0 & 0\,0\,0\,0\,0\,0\,0\,0\,0\,0\,0\,0\,0\,0\,0 & 0\,0\,0\,0\,0\,0 \\
1/2 & 0\,0 & 0\,0\,0\,0\,0\,0\,0\,0\,0 & 0\,0\,0\,0\,0\,0 & 0\,0\,0\,0\,0\,0\,0\,0\,0\,0\,0\,0\,0\,0\,0 & 0\,0\,0\,0\,0\,0 \\
1/2 & 0\,0 & 0\,0\,0\,0\,0\,0\,0\,0\,0 & 0\,0\,0\,0\,0\,0 & 0\,0\,0\,0\,0\,0\,0\,0\,0\,0\,0\,0\,0\,0\,0 & 0\,0\,0\,0\,0\,0
\end{pmatrix}
\end{aligned}
\tag{110}
$$

The ICM_1 contains the resulting ICVs as its row vectors, so that the $[\theta]_1$- and the $[\theta]_2$-rows are identical with the vectors shown in Eqs. 88 and 89.

The value $\frac{1}{2}$ at the intersection between the $[\theta]_3$-row and $\mathbf{C}_{3\tilde{\sigma}}$-column (the 17th column) in the ICM_1 (Eq. 110) corresponds to the term $\frac{1}{2}\,(\mathrm{A}^3\mathrm{p}+\mathrm{A}^3\overline{\mathrm{p}})$, which indicates that an enantiomeric pair is counted once.

For an additional example, let us consider an FPM corresponding to the following partitions:

$$[\theta]_{20} = [0, 0, 0, 0; 4, 0, 0, 0, 0, 0, 0, 0] \quad (\text{for } \mathrm{p}^4 \text{ etc.}) \tag{111}$$
$$[\theta]_{21} = [0, 0, 0, 0; 3, 1, 0, 0, 0, 0, 0, 0] \quad (\text{for } \mathrm{p}^3\overline{\mathrm{p}} \text{ etc.}) \tag{112}$$
$$[\theta]_{22} = [0, 0, 0, 0; 3, 0, 1, 0, 0, 0, 0, 0] \quad (\text{for } \mathrm{p}^3\mathrm{q} \text{ etc.}) \tag{113}$$
$$[\theta]_{23} = [0, 0, 0, 0; 2, 2, 0, 0, 0, 0, 0, 0] \quad (\text{for } \mathrm{p}^2\overline{\mathrm{p}}^2 \text{ etc.}) \tag{114}$$
$$[\theta]_{24} = [0, 0, 0, 0; 2, 1, 1, 0, 0, 0, 0, 0] \quad (\text{for } \mathrm{p}^2\overline{\mathrm{p}}\mathrm{q} \text{ etc.}) \tag{115}$$
$$[\theta]_{25} = [0, 0, 0, 0; 2, 0, 2, 0, 0, 0, 0, 0] \quad (\text{for } \mathrm{p}^2\mathrm{q}^2 \text{ etc.}) \tag{116}$$
$$[\theta]_{26} = [0, 0, 0, 0; 2, 0, 1, 1, 0, 0, 0, 0] \quad (\text{for } \mathrm{p}^2\mathrm{q}\overline{\mathrm{q}} \text{ etc.}) \tag{117}$$
$$[\theta]_{27} = [0, 0, 0, 0; 2, 0, 1, 0, 1, 0, 0, 0] \quad (\text{for } \mathrm{p}^2\mathrm{qr} \text{ etc.}) \tag{118}$$
$$[\theta]_{28} = [0, 0, 0, 0; 1, 1, 1, 1, 0, 0, 0, 0] \quad (\text{for } \mathrm{p}\overline{\mathrm{p}}\mathrm{q}\overline{\mathrm{q}} \text{ etc.}) \tag{119}$$
$$[\theta]_{29} = [0, 0, 0, 0; 1, 1, 1, 0, 1, 0, 0, 0] \quad (\text{for } \mathrm{p}\overline{\mathrm{p}}\mathrm{qr} \text{ etc.}) \tag{120}$$
$$[\theta]_{30} = [0, 0, 0, 0; 1, 0, 1, 0, 1, 0, 1, 0] \quad (\text{for pqrs etc.}) \tag{121}$$

The FPM can be constructed from the data of generating functions (e.g., Eq. 81) by applying the procedure described above:

$$
\begin{array}{rl}
 & \mathrm{FPM}_2 \\
 & \begin{array}{r} [\theta]_{20} \\ [\theta]_{21} \\ [\theta]_{22} \\ [\theta]_{23} \\ [\theta]_{24} \\ [\theta]_{25} \\ [\theta]_{26} \\ [\theta]_{27} \\ [\theta]_{28} \\ [\theta]_{29} \\ [\theta]_{30} \end{array}
\begin{pmatrix}
1 & 1 & 1 & 0 & 0 & 0 & 1 & 1 & 0 & 1 & 1 & 0 & 0 & 0 & 0 & 0 & 1 & 0 & 0 & 1 & 0 & 0 & 0 & 0 & 0 & 0 & 1 & 0 & 0 & 1 & 0 & 0 & 0 \\
4 & 0 & 2 & 0 & 0 & 0 & 1 & 0 & 0 & 0 & 0 & 0 & 0 & 0 & 0 & 0 & 1 & 0 & 0 & 0 & 0 & 0 & 0 & 0 & 0 & 0 & 0 & 0 & 0 & 0 & 0 & 0 & 0 \\
4 & 0 & 2 & 0 & 0 & 0 & 1 & 0 & 0 & 0 & 0 & 0 & 0 & 0 & 0 & 0 & 1 & 0 & 0 & 0 & 0 & 0 & 0 & 0 & 0 & 0 & 0 & 0 & 0 & 0 & 0 & 0 & 0 \\
6 & 2 & 2 & 4 & 0 & 0 & 0 & 0 & 2 & 0 & 2 & 2 & 0 & 0 & 0 & 0 & 0 & 0 & 0 & 0 & 0 & 0 & 0 & 2 & 0 & 0 & 0 & 0 & 0 & 0 & 0 & 0 & 0 \\
12 & 0 & 2 & 0 & 0 & 0 & 0 & 0 & 0 & 0 & 0 & 0 & 0 & 0 & 0 & 0 & 0 & 0 & 0 & 0 & 0 & 0 & 0 & 0 & 0 & 0 & 0 & 0 & 0 & 0 & 0 & 0 & 0 \\
6 & 2 & 2 & 0 & 0 & 0 & 0 & 0 & 0 & 0 & 2 & 0 & 0 & 0 & 0 & 0 & 0 & 0 & 0 & 0 & 0 & 0 & 0 & 0 & 0 & 0 & 0 & 0 & 0 & 0 & 0 & 0 & 0 \\
12 & 0 & 2 & 0 & 0 & 0 & 0 & 0 & 0 & 0 & 0 & 0 & 0 & 0 & 0 & 0 & 0 & 0 & 0 & 0 & 0 & 0 & 0 & 0 & 0 & 0 & 0 & 0 & 0 & 0 & 0 & 0 & 0 \\
12 & 0 & 2 & 0 & 0 & 0 & 0 & 0 & 0 & 0 & 0 & 0 & 0 & 0 & 0 & 0 & 0 & 0 & 0 & 0 & 0 & 0 & 0 & 0 & 0 & 0 & 0 & 0 & 0 & 0 & 0 & 0 & 0 \\
24 & 0 & 0 & 8 & 0 & 0 & 0 & 0 & 0 & 0 & 0 & 0 & 0 & 0 & 0 & 0 & 0 & 0 & 0 & 0 & 0 & 0 & 0 & 0 & 0 & 0 & 0 & 0 & 0 & 0 & 0 & 0 & 0 \\
24 & 0 & 0 & 0 & 0 & 0 & 0 & 0 & 0 & 0 & 0 & 0 & 0 & 0 & 0 & 0 & 0 & 0 & 0 & 0 & 0 & 0 & 0 & 0 & 0 & 0 & 0 & 0 & 0 & 0 & 0 & 0 & 0 \\
24 & 0 & 0 & 0 & 0 & 0 & 0 & 0 & 0 & 0 & 0 & 0 & 0 & 0 & 0 & 0 & 0 & 0 & 0 & 0 & 0 & 0 & 0 & 0 & 0 & 0 & 0 & 0 & 0 & 0 & 0 & 0 & 0
\end{pmatrix}
\end{array}
\tag{122}
$$

The FPM (Eq. 53) is multiplied by $M^{-1}_{\mathbf{T}_{d\tilde{\sigma}\hat{I}}}$ (Eq. 4.2), so as to give another isomer-counting matrix (ICM_2):

$$
\begin{array}{rl}
\mathrm{ICM}_2 = \mathrm{FPM}_2 \times M^{-1}_{\mathbf{T}_{d\tilde{\sigma}\hat{I}}} & \\
 & \begin{array}{r} [\theta]_{20} \\ [\theta]_{21} \\ [\theta]_{22} \\ [\theta]_{23} \\ [\theta]_{24} \\ [\theta]_{25} \\ [\theta]_{26} \\ [\theta]_{27} \\ [\theta]_{28} \\ [\theta]_{29} \\ [\theta]_{30} \end{array}
\begin{pmatrix}
0 & 0 & 0 & 0 & 0 & 0 & 0 & 0 & 0 & 0 & 0 & 0 & 0 & 0 & 0 & 0 & 0 & 0 & 0 & 0 & 0 & 0 & 0 & 0 & 0 & 0 & 0 & 0 & 0 & 0 & 1/2 & 0 & 0 & 0 \\
0 & 0 & 0 & 0 & 0 & 0 & 0 & 0 & 0 & 0 & 0 & 0 & 0 & 0 & 0 & 0 & 0 & 1/2 & 0 & 0 & 0 & 0 & 0 & 0 & 0 & 0 & 0 & 0 & 0 & 0 & 0 & 0 & 0 \\
0 & 0 & 0 & 0 & 0 & 0 & 0 & 0 & 0 & 0 & 0 & 0 & 0 & 0 & 0 & 0 & 0 & 1/2 & 0 & 0 & 0 & 0 & 0 & 0 & 0 & 0 & 0 & 0 & 0 & 0 & 0 & 0 & 0 \\
0 & 0 & 0 & 0 & 0 & 0 & 0 & 0 & 0 & 0 & 0 & 0 & 0 & 0 & 0 & 0 & 0 & 0 & 0 & 0 & 0 & 0 & 0 & 1 & 0 & 0 & 0 & 0 & 0 & 0 & 0 & 0 & 0 \\
0 & 0 & 1/2 & 0 & 0 & 0 & 0 & 0 & 0 & 0 & 0 & 0 & 0 & 0 & 0 & 0 & 0 & 0 & 0 & 0 & 0 & 0 & 0 & 0 & 0 & 0 & 0 & 0 & 0 & 0 & 0 & 0 & 0 \\
0 & 0 & 0 & 0 & 0 & 0 & 0 & 0 & 0 & 1/2 & 0 & 0 & 0 & 0 & 0 & 0 & 0 & 0 & 0 & 0 & 0 & 0 & 0 & 0 & 0 & 0 & 0 & 0 & 0 & 0 & 0 & 0 & 0 & 0 \\
0 & 0 & 1/2 & 0 & 0 & 0 & 0 & 0 & 0 & 0 & 0 & 0 & 0 & 0 & 0 & 0 & 0 & 0 & 0 & 0 & 0 & 0 & 0 & 0 & 0 & 0 & 0 & 0 & 0 & 0 & 0 & 0 & 0 \\
0 & 0 & 1/2 & 0 & 0 & 0 & 0 & 0 & 0 & 0 & 0 & 0 & 0 & 0 & 0 & 0 & 0 & 0 & 0 & 0 & 0 & 0 & 0 & 0 & 0 & 0 & 0 & 0 & 0 & 0 & 0 & 0 & 0 & 0 \\
0 & 0 & 0 & 1 & 0 & 0 & 0 & 0 & 0 & 0 & 0 & 0 & 0 & 0 & 0 & 0 & 0 & 0 & 0 & 0 & 0 & 0 & 0 & 0 & 0 & 0 & 0 & 0 & 0 & 0 & 0 & 0 & 0 & 0 \\
1/2 & 0 & 0 & 0 & 0 & 0 & 0 & 0 & 0 & 0 & 0 & 0 & 0 & 0 & 0 & 0 & 0 & 0 & 0 & 0 & 0 & 0 & 0 & 0 & 0 & 0 & 0 & 0 & 0 & 0 & 0 & 0 & 0 & 0 \\
1/2 & 0 & 0 & 0 & 0 & 0 & 0 & 0 & 0 & 0 & 0 & 0 & 0 & 0 & 0 & 0 & 0 & 0 & 0 & 0 & 0 & 0 & 0 & 0 & 0 & 0 & 0 & 0 & 0 & 0 & 0 & 0 & 0 & 0
\end{pmatrix}
\end{array}
\tag{123}
$$

The results of the itemized enumeration (Eqs. 110 and 123) are illustrated in Fig. 9, which is a modification of Fig. 3 of [41]. Each promolecule (as a representative of a quadruplet for a stereoisogram) is selected to be a representative of promolecules (representatives of quadruplets) with a given partition and accompanied with the information on its *RS*-stereoisomeric group, its point group, and its stereoisogram type. For example, the promolecule **16** with ABXY is a representative of the partition $[\theta]_{10}$, which is characterized by the *RS*-stereoisomeric group $\mathbf{C}_{\hat{I}}$, the point group $\mathbf{C}_1$, and a type-I stereoisogram. Note that each promolecule corresponds to a respective stereoisogram (cf. Fig. 2 of [41]). The categorization of *RS*-stereoisomeric groups to stereoisogram types are summarized in Fig. 8.

	RS-astereogenic	*RS*-stereogenic
chiral		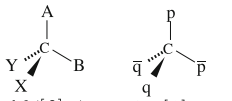 **16** ($[\theta]_{10}$) $\mathbf{C}_{\widehat{I}}$, $\mathbf{C}_1$, I **17** ($[\theta]_{28}$) $\mathbf{C}_{\widehat{\sigma}}$, $\mathbf{C}_1$, I
	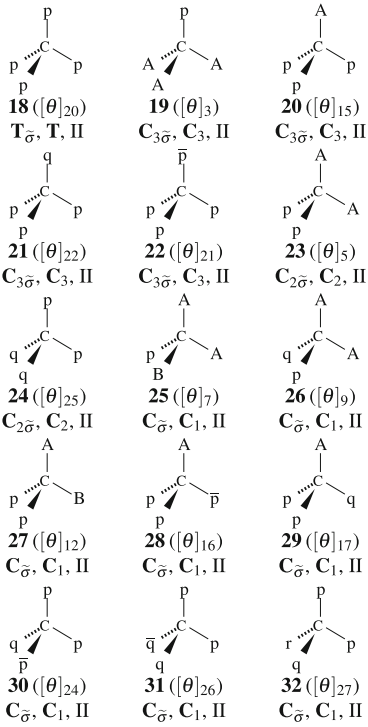 **18** ($[\theta]_{20}$) $\mathbf{T}_{\widetilde{\sigma}}$, **T**, II **19** ($[\theta]_3$) $\mathbf{C}_{3\widetilde{\sigma}}$, $\mathbf{C}_3$, II **20** ($[\theta]_{15}$) $\mathbf{C}_{3\widetilde{\sigma}}$, $\mathbf{C}_3$, II **21** ($[\theta]_{22}$) $\mathbf{C}_{3\widetilde{\sigma}}$, $\mathbf{C}_3$, II **22** ($[\theta]_{21}$) $\mathbf{C}_{3\widetilde{\sigma}}$, $\mathbf{C}_3$, II **23** ($[\theta]_5$) $\mathbf{C}_{2\widetilde{\sigma}}$, $\mathbf{C}_2$, II **24** ($[\theta]_{25}$) $\mathbf{C}_{2\widetilde{\sigma}}$, $\mathbf{C}_2$, II **25** ($[\theta]_7$) $\mathbf{C}_{\widetilde{\sigma}}$, $\mathbf{C}_1$, II **26** ($[\theta]_9$) $\mathbf{C}_{\widetilde{\sigma}}$, $\mathbf{C}_1$, II **27** ($[\theta]_{12}$) $\mathbf{C}_{\widetilde{\sigma}}$, $\mathbf{C}_1$, II **28** ($[\theta]_{16}$) $\mathbf{C}_{\widetilde{\sigma}}$, $\mathbf{C}_1$, II **29** ($[\theta]_{17}$) $\mathbf{C}_{\widetilde{\sigma}}$, $\mathbf{C}_1$, II **30** ($[\theta]_{24}$) $\mathbf{C}_{\widetilde{\sigma}}$, $\mathbf{C}_1$, II **31** ($[\theta]_{26}$) $\mathbf{C}_{\widetilde{\sigma}}$, $\mathbf{C}_1$, II **32** ($[\theta]_{27}$) $\mathbf{C}_{\widetilde{\sigma}}$, $\mathbf{C}_1$, II	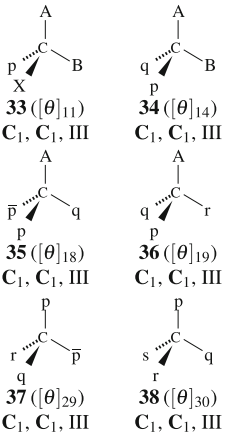 **33** ($[\theta]_{11}$) $\mathbf{C}_1$, $\mathbf{C}_1$, III **34** ($[\theta]_{14}$) $\mathbf{C}_1$, $\mathbf{C}_1$, III **35** ($[\theta]_{18}$) $\mathbf{C}_1$, $\mathbf{C}_1$, III **36** ($[\theta]_{19}$) $\mathbf{C}_1$, $\mathbf{C}_1$, III **37** ($[\theta]_{29}$) $\mathbf{C}_1$, $\mathbf{C}_1$, III **38** ($[\theta]_{30}$) $\mathbf{C}_1$, $\mathbf{C}_1$, III
achiral	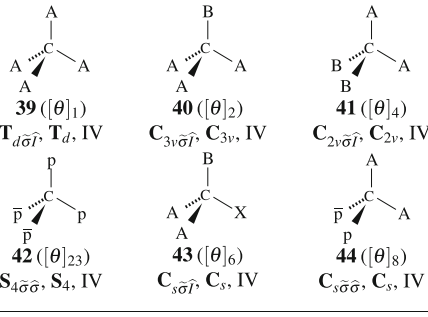 **39** ($[\theta]_1$) $\mathbf{T}_{d\widetilde{\sigma}\widehat{I}}$, $\mathbf{T}_d$, IV **40** ($[\theta]_2$) $\mathbf{C}_{3v\widetilde{\sigma}\widehat{I}}$, $\mathbf{C}_{3v}$, IV **41** ($[\theta]_4$) $\mathbf{C}_{2v\widetilde{\sigma}\widehat{I}}$, $\mathbf{C}_{2v}$, IV **42** ($[\theta]_{23}$) $\mathbf{S}_{4\widetilde{\sigma}\widehat{\sigma}}$, $\mathbf{S}_4$, IV **43** ($[\theta]_6$) $\mathbf{C}_{s\widetilde{\sigma}\widehat{I}}$, $\mathbf{C}_s$, IV **44** ($[\theta]_8$) $\mathbf{C}_{s\widetilde{\sigma}\widehat{\sigma}}$, $\mathbf{C}_s$, IV	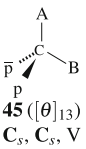 **45** ($[\theta]_{13}$) $\mathbf{C}_s$, $\mathbf{C}_s$, V

Fig. 9 Quadruplets of *RS*-Stereoisomers (Types I–V) for tetrahedral promolecules. The symbols A, B, X, and Y represent atoms or achiral ligands. The symbols p, q, r, and s represents chiral ligands, while each symbol with an overbar represents the corresponding chiral ligand with the opposite chirality. An arbitrary promolecule is depicted as a representative of each quadruplet of *RS*-stereoisomers. The compound number (its partition), its *RS*-stereoisomeric group, its point group, and its stereoisogram type are attached to each promolecule

6 Type-itemized enumeration

6.1 Type-enumeration matrices

As shown in Fig. 8, the 33 subgroups of the *RS*-stereoisomeric group $\mathbf{T}_{d\tilde{\sigma}\hat{I}}$ are categorized into five types represented by the following sets:

$$\text{Type I: } \mathrm{SG}^{[\mathrm{I}]} = \{\overset{4}{\mathbf{C}}_{\tilde{\sigma}}, \overset{6}{\mathbf{C}}_{\hat{I}}, \overset{12}{\mathbf{C}}_{2\hat{\sigma}}, \overset{15}{\mathbf{C}}_{2\hat{I}}, \overset{19}{\mathbf{C}}_{3\hat{I}}, \overset{25}{\mathbf{D}}_{2\hat{I}}, \overset{31}{\mathbf{T}}_{\hat{I}}\} \tag{124}$$

$$\text{Type II: } \mathrm{SG}^{[\mathrm{II}]} = \{\overset{3}{\mathbf{C}}_{\tilde{\sigma}}, \overset{8}{\mathbf{S}}_{\tilde{4}}, \overset{11}{\mathbf{C}}_{2\tilde{\sigma}}, \overset{17}{\mathbf{C}}_{3\tilde{\sigma}}, \overset{20}{\mathbf{D}}_{2\tilde{\sigma}}, \overset{30}{\mathbf{T}}_{\tilde{\sigma}}\} \tag{125}$$

$$\text{Type III: } \mathrm{SG}^{[\mathrm{III}]} = \{\overset{1}{\mathbf{C}}_{1}, \overset{2}{\mathbf{C}}_{2}, \overset{7}{\mathbf{C}}_{3}, \overset{10}{\mathbf{D}}_{2}, \overset{27}{\mathbf{T}}\} \tag{126}$$

$$\text{Type IV: } \mathrm{SG}^{[\mathrm{IV}]} = \{\overset{14}{\mathbf{C}}_{s\tilde{\sigma}\hat{\sigma}}, \overset{16}{\mathbf{C}}_{s\tilde{\sigma}\hat{I}}, \overset{21}{\mathbf{S}}_{\tilde{4}\hat{\sigma}}, \overset{22}{\mathbf{S}}_{\tilde{4}\hat{I}}, \overset{24}{\mathbf{S}}_{4\tilde{\sigma}\hat{\sigma}}, \overset{26}{\mathbf{C}}_{2v\tilde{\sigma}\hat{I}}, \overset{28}{\mathbf{C}}_{3v\tilde{\sigma}\hat{I}}, \overset{29}{\mathbf{D}}_{2d\tilde{\sigma}\hat{I}}, \overset{33}{\mathbf{T}}_{d\tilde{\sigma}\hat{I}}\} \tag{127}$$

$$\text{Type V: } \mathrm{SG}^{[\mathrm{V}]} = \{\overset{5}{\mathbf{C}}_{s}, \overset{9}{\mathbf{S}}_{4}, \overset{13}{\mathbf{C}}_{2v}, \overset{18}{\mathbf{C}}_{3v}, \overset{23}{\mathbf{D}}_{2d}, \overset{32}{\mathbf{T}}_{d}\}. \tag{128}$$

Each of the tetrahedral promolecules collected in Fig. 9 is a representative ($\mathbf{A}$, $\overline{\mathbf{A}}$, $\mathbf{B}$, or $\overline{\mathbf{B}}$) of a quadruplet which constructs a stereoisogram shown in Fig. 10. The subgroups of $\mathbf{T}_{d\tilde{\sigma}\hat{I}}$ for characterizing respective types are shown along with three attributes. For the three attributes and the related three relationships, see [17] and [41].

Let $\overline{m}_{ji}$ be the ji-element of the inverse mark table $M^{-1}_{\mathbf{T}_{d\tilde{\sigma}\hat{I}}}$ (Eq. 4.2). The $\acute{\mathbf{G}}_j$-row is tentatively fixed and the row is summed up according to the categorization of type I–V as follows:

$$\widehat{N}_j^{(I)} = \sum_{\acute{\mathbf{G}}_i \in \mathrm{SG}^{[\mathrm{I}]}} \overline{m}_{ji} \tag{129}$$

$$\widehat{N}_j^{(II)} = \sum_{\acute{\mathbf{G}}_i \in \mathrm{SG}^{[\mathrm{II}]}} \overline{m}_{ji} \tag{130}$$

$$\widehat{N}_j^{(III)} = \sum_{\acute{\mathbf{G}}_i \in \mathrm{SG}^{[\mathrm{III}]}} \overline{m}_{ji} \tag{131}$$

$$\widehat{N}_j^{(IV)} = \sum_{\acute{\mathbf{G}}_i \in \mathrm{SG}^{[\mathrm{IV}]}} \overline{m}_{ji} \tag{132}$$

$$\widehat{N}_j^{(V)} = \sum_{\acute{\mathbf{G}}_i \in \mathrm{SG}^{[\mathrm{V}]}} \overline{m}_{ji} \tag{133}$$

$$\widehat{N}_j = \widehat{N}_j^{(I)} + \widehat{N}_j^{(II)} + \widehat{N}_j^{(III)} + \widehat{N}_j^{(IV)} + \widehat{N}_j^{(V)} \tag{134}$$

In a parallel way to a gross-enumeration matrix GEM for gross enumerations [cf. Table 2 of the present paper and Eq. 48 of [42]], let us consider a 33×6 type-enumeration matrix TEM for type-itemized enumerations, where the jth row (TEM_j) as a row vector is represented as follows:

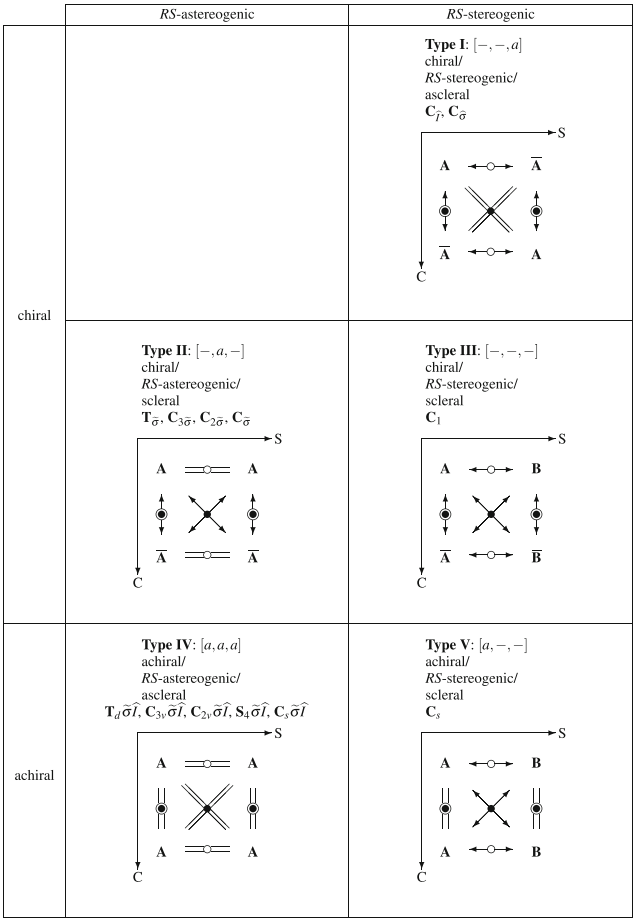

symbol	relationship	attribute
⟷	enantiomeric	chiral
⟷	(self-enantiomeric)	achiral
⟷	*RS*-diastereomeric	*RS*-stereogenic
⟷	(self-*RS*-diastereomeric)	*RS*-astereogenic
⟷	holantimeric	scleral
⟷	(self-holantimeric)	ascleral

Fig. 10 Stereoisograms for representing *RS*-stereoisomers of five types. This figure is a modification of Fig. 6 of [17] and of Fig. 6 of [41], where the subgroups of $\mathbf{T}_{d\tilde{\sigma}\hat{I}}$ for characterizing respective types are shown along with three attributes. The symbols **A** and $\overline{\mathbf{A}}$ (or **B** and $\overline{\mathbf{B}}$) represent a pair of enantiomers based on a tetrahedral skeleton, where the **A** at the *upper-left* position of each stereoisogram is selected from the promolecules listed in Fig. 9

$$\mathrm{TEM}_j = \left(\widehat{N}_j, \widehat{N}_j^{(I)}, \widehat{N}_j^{(II)}, \widehat{N}_j^{(III)}, \widehat{N}_j^{(IV)}, \widehat{N}_j^{(V)}\right) \tag{135}$$

for $\acute{\mathbf{G}}_j$ ($\in \mathrm{SSG}_{\mathbf{T}_{d\tilde{\sigma}\hat{I}}}$) (cf. Eq. 51). The respective elements of TEM_j are collected in Table 3. The elements of TEM_j are consistent with the coefficients appearing in the

cycle indices with chirality fittingness (CI-CFs) reported previously [i.e., Eqs. 83 (for type I), 84 (for type II), 85 (for type III), 81 (for type IV), and 82 (for type V) of [41]], which were obtained by an alternative way.

Because the FPM_1 (Eq. 109) contains FPVs as its row vectors, it is multiplied by the TEM (Eq. 135 and Table 3) so as to give an isomer-type-counting matrix (ITCM), where the six columns contain the numbers of total quadruplets and those of quadruplets of the respective types.

$$\mathrm{ITCM}_1 = \mathrm{FPM}_1 \times \mathrm{TEM} = \begin{array}{c} \\ [\theta]_1 \\ [\theta]_2 \\ [\theta]_3 \\ [\theta]_4 \\ [\theta]_5 \\ [\theta]_6 \\ [\theta]_7 \\ [\theta]_8 \\ [\theta]_9 \\ [\theta]_{10} \\ [\theta]_{11} \\ [\theta]_{12} \\ [\theta]_{13} \\ [\theta]_{14} \\ [\theta]_{15} \\ [\theta]_{16} \\ [\theta]_{17} \\ [\theta]_{18} \\ [\theta]_{19} \end{array} \begin{pmatrix} 1 & 0 & 0 & 0 & 1 & 0 \\ 1 & 0 & 0 & 0 & 1 & 0 \\ 1/2 & 0 & 1/2 & 0 & 0 & 0 \\ 1 & 0 & 0 & 0 & 1 & 0 \\ 1/2 & 0 & 1/2 & 0 & 0 & 0 \\ 1 & 0 & 0 & 0 & 1 & 0 \\ 1/2 & 0 & 1/2 & 0 & 0 & 0 \\ 1 & 0 & 0 & 0 & 1 & 0 \\ 1/2 & 0 & 1/2 & 0 & 0 & 0 \\ 1 & 1 & 0 & 0 & 0 & 0 \\ 1/2 & 0 & 0 & 1/2 & 0 & 0 \\ 1/2 & 0 & 1/2 & 0 & 0 & 0 \\ 1 & 0 & 0 & 0 & 0 & 1 \\ 1/2 & 0 & 0 & 1/2 & 0 & 0 \\ 1/2 & 0 & 1/2 & 0 & 0 & 0 \\ 1/2 & 0 & 1/2 & 0 & 0 & 0 \\ 1/2 & 0 & 1/2 & 0 & 0 & 0 \\ 1/2 & 0 & 0 & 1/2 & 0 & 0 \\ 1/2 & 0 & 0 & 1/2 & 0 & 0 \end{pmatrix} \tag{136}$$

These values are consistent with the quadruplets listed in Fig. 9. For example, the value 1/2 at the intersection of the $[\theta]_3$-row and the third column (the type-II column) in Eq. 136 corresponds to the term $\frac{1}{2}(\mathrm{A}^3\mathrm{p} + \mathrm{A}^3\overline{\mathrm{p}})$. This term indicates the presence of a quadruplet of *RS*-stereoisomers (as a pair of enantiomers) with the partition $[\theta]_3$, where the $\mathbf{C}_{3\widetilde{\sigma}}$-promolecule **19** is a representative of the quadruplet characterized by the type-II stereoisogram shown in Fig. 10.

In a similar way, the FPM_2 (Eq. 122) contains FPVs as its row vectors. The matrix is multiplied by the TEM (Eq. 135 and Table 3) so as to give an isomer-type-counting matrix (ITCM), where the six columns contain the numbers of total quadruplets and of quadruplets of respective types.

$$\mathrm{ITCM}_2 = \mathrm{FPM}_2 \times \mathrm{TEM} = \begin{matrix}[\theta]_{20}\\ [\theta]_{21}\\ [\theta]_{22}\\ [\theta]_{23}\\ [\theta]_{24}\\ [\theta]_{25}\\ [\theta]_{26}\\ [\theta]_{27}\\ [\theta]_{28}\\ [\theta]_{29}\\ [\theta]_{30}\end{matrix} \begin{pmatrix} 1/2 & 0 & 1/2 & 0 & 0 & 0\\ 1/2 & 0 & 1/2 & 0 & 0 & 0\\ 1/2 & 0 & 1/2 & 0 & 0 & 0\\ 1 & 0 & 0 & 0 & 1 & 0\\ 1/2 & 0 & 1/2 & 0 & 0 & 0\\ 1/2 & 0 & 1/2 & 0 & 0 & 0\\ 1/2 & 0 & 1/2 & 0 & 0 & 0\\ 1/2 & 0 & 1/2 & 0 & 0 & 0\\ 1 & 1 & 0 & 0 & 0 & 0\\ 1/2 & 0 & 0 & 1/2 & 0 & 0\\ 1/2 & 0 & 0 & 1/2 & 0 & 0 \end{pmatrix} \tag{137}$$

These values are consistent with the quadruplets listed in Fig. 9. In addition, the values calculated in Eqs. 136 and 137 are consistent with the previous results calculated by an alternative method [41]: the second columns of Eqs. 136 and 137 (type I) is consistent with Eq. 86 of [41], the third columns (type II) with Eq. 87 of [41], the 4th columns (type III) with Eq. 88 of [41], the 5th columns (type IV) with Eq. 89 of [41], and the 6th columns (type V) with Eq. 90 of [41].

7 Conclusion

After the isomorphism between the *RS*-stereoisomeric group $\mathbf{T}_{d\tilde{\sigma}\hat{I}}$ and the point group $\mathbf{O}_h$ has been throughly discussed, unit-subduced cycle indices with chirality fittingness (USCI-CFs) for characterizing $\mathbf{T}_{d\tilde{\sigma}\hat{I}}$ are obtained according to the USCI approach developed by Fujita [44]. Then, the fixed-point matrix (FPM) method of the USCI approach is applied to the USCI-CFs. Thereby, the numbers of quadruplets are calculated in an itemized fashion with respect to the subgroups of $\mathbf{T}_{d\tilde{\sigma}\hat{I}}$. After the subgroups of $\mathbf{T}_{d\tilde{\sigma}\hat{I}}$ are categorized into types I–V, type-itemized enumeration of quadruplets is conducted to illustrate the versatility of the stereoisogram approach.

References

1. IUPAC Organic Chemistry Division, Pure Appl. Chem. **68**, 2193–2222 (1996)
2. K. Mislow, Chirality **14**, 126–134 (2002)
3. E.L. Eliel, S.H. Wilen, *Stereochemistry of Organic Compounds* (Wiley, New York, 1994)
4. N. North, *Principles and Applications of Stereochemistry* (Stanley Thornes, Cheltenham, 1998)
5. D.G. Morris, *Stereochemistry* (Royal Society of Chemistry, Cambridge, 2001)
6. T.W.G. Solomons, *Organic Chemistry*, 3rd edn. (Wiley, New York, 1984)
7. R.J. Fessenden, J.S. Fessenden, *Organic Chemistry*, 3rd edn. (Brooks/Cole, Monterey, 1986)
8. S.H. Pine, *Organic Chemistry*, 5th edn. (McGraw-Hill, New York, 1987)
9. R.T. Morrison, R.N. Boyd, *Organic Chemistry*, 5th edn. (Allyn and Bacon, Boston, 1987)
10. K.P.C. Vollhardt, N.E. Schore, *Organic Chemistry: Structure and Function*, 4th edn. (Freeman, New York, 2003)
11. R.S. Cahn, C.K. Ingold, V. Prelog, Angew. Chem. Int. Ed. Eng. **5**, 385–415 (1966)
12. V. Prelog, G. Helmchen, Angew. Chem. Int. Ed. Eng. **21**, 567–583 (1982)
13. K.R. Hanson, J. Am. Chem. Soc. **88**, 2731–2742 (1966)
14. S. Fujita, Tetrahedron **47**, 31–46 (1991)
15. S. Fujita, J. Org. Chem. **69**, 3158–3165 (2004)

16. S. Fujita, J. Math. Chem. **35**, 265–287 (2004)
17. S. Fujita, Tetrahedron **60**, 11629–11638 (2004)
18. S. Fujita, MATCH Commun. Math. Comput. Chem. **61**, 11–38 (2009)
19. S. Fujita, J. Comput. Aided Chem. **10**, 16–29 (2009)
20. S. Fujita, Stereoisograms: A Remedy Against Oversimplified Dichotomy between Enantiomers and Diastereomers in Stereochemistry, in *Chemical Information and Computational Challenge in the 21st Chentury*, ed. by M. V. Putz (Nova, New York 2012), Chapter 9, pp. 223–242
21. S. Fujita, Tetrahedron **62**, 691–705 (2006)
22. S. Fujita, Yuki Gosei Kagaku Kyokai-Shi. J. Synth. Org. Chem. Jpn. **66**, 995–1004 (2008)
23. S. Fujita, MATCH Commun. Math. Comput. Chem. **61**, 39–70 (2009)
24. S. Fujita, J. Comput. Aided Chem. **10**, 76–95 (2009)
25. S. Fujita, Prochirality and pro-RS-stereogenicity. Stereoisogram Approach Free from the Conventional "Prochirality" and "Prostereogenicity", in *Carbon Bonding and Structures. Advances in Physics and Chemistry*, ed. by M. V. Putz, (Springer, Dordrecht, Heidelberg, London) Vol. 5 of Carbon Materials: Chemistry and Physics. Chapter 10, pp. 227–271 (2011)
26. S. Fujita, MATCH Commun. Math. Comput. Chem. **52**, 3–18 (2004)
27. S. Fujita, Memoirs of the faculty of engineering and design. Kyoto Inst. Technol. **53**, 19–38 (2005)
28. S. Fujita, MATCH Commun. Math. Comput. Chem. **53**, 147–159 (2005)
29. S. Fujita, J. Chem. Inf. Comput. Sci. **44**, 1719–1726 (2004)
30. S. Fujita, J. Math. Chem. **50**, 1791–1814 (2012)
31. S. Fujita, J. Math. Chem. **50**, 1815–1860 (2012)
32. S. Fujita, J. Math. Chem. **50**, 2202–2222 (2012)
33. S. Fujita, J. Math. Chem. **50**, 2168–2201 (2012)
34. S. Fujita, MATCH Commun. Math. Comput. Chem. **54**, 39–52 (2005)
35. S. Fujita, MATCH Commun. Math. Comput. Chem. **63**, 3–24 (2010)
36. S. Fujita, MATCH Commun. Math. Comput. Chem. **63**, 25–66 (2010)
37. S. Fujita, J. Math. Chem. **47**, 145–166 (2010)
38. S. Fujita, Tetrahedron **65**, 1581–1592 (2009)
39. S. Fujita, J. Math. Chem. **49**, 95–162 (2011)
40. S. Fujita, Tetrahedron: Asymmetry **23**, 623–634 (2012)
41. S. Fujita, MATCH Commun. Math. Comput. Chem. **61**, 71–115 (2009)
42. S. Fujita, Bull. Chem. Soc. Jpn. **84**, 1192–1207 (2011)
43. S. Fujita, Bull. Chem. Soc. Jpn. **85**, 793–810 (2012)
44. S. Fujita, *Symmetry and combinatorial enumeration in chemistry* (Springer, Berlin, 1991)
45. S. Fujita, *Diagrammatical Approach to Molecular Symmetry and Enumeration of Stereoisomers* (University of Kragujevac, Faculty of Science, Kragujevac, 2007)
46. S. Fujita, *Combinatorial Enumeration of Graphs, Three-Dimensional Structures, and Chemical Compounds* (University of Kragujevac, Faculty of Science, Kragujevac, 2013)
47. S. Fujita, Polyhedron **12**, 95–110 (1993)